REPORT DOCUMENTATION PAGE

Form Approved
OMB No. 0704-0188

PLEASE DO NOT RETURN YOUR FORM TO THE ABOVE ORGANIZATION.

1. REPORT DATE *(DD-MM-YYYY)*	2. REPORT TYPE	3. DATES COVERED *(From - To)*
25-01-2012	Final Progress Report	March 2004-Dec 2011

4. TITLE AND SUBTITLE
Correlation Between Physicochemical Characteristics and Toxicological Properties of Nanomaterials

5a. CONTRACT NUMBER

5b. GRANT NUMBER
FA9550-04-1-0430

5c. PROGRAM ELEMENT NUMBER
61103F

6. AUTHOR(S)
Günter Oberdörster, Alison Elder, Jacob Finkelstein, Thomas Gunter, Jim McGrath, Todd Krauss , Lisa DeLouise, Amber Rinderknecht, Zhihui Ban
David Pui , Chen, Da-Ren, Kim, Seong Chan, Qi, Chaolong
Pratim Biswas, Daren Chen, Zhu Liying, Chen Xu , Jiang Jingkun, Sahu, Manoranjan, Fan Mei

5d. PROJECT NUMBER

5e. TASK NUMBER

5f. WORK UNIT NUMBER

7. PERFORMING ORGANIZATION NAME(S) AND ADDRESS(ES)
University of Rochester, Department of Environmental Medicine, 575 Elmwood Avenue,Medical Center Box 850, Rochester, NY 14642. University of Minnesota, Mechanical Engineering, 111 Church St SE., Department of Chemical Engineering, Washington University in St. Louis, One Brookings Drive, Campus Box 1180

8. PERFORMING ORGANIZATION REPORT NUMBER

9. SPONSORING/MONITORING AGENCY NAME(S) AND ADDRESS(ES)
University of Rochester, Department of Environmental Medicine, 575 Elmwood Avenue,Medical Center Box 850, Rochester, NY 14642. University of Minnesota, Mechanical Engineering, 111 Church St SE., Department of Chemical Engineering, Washington University in St. Louis, One Brookings Drive, Campus Box 1180

10. SPONSOR/MONITOR'S ACRONYM(S)
AFOSR

11. SPONSOR/MONITOR'S REPORT NUMBER(S)
AFRL-OSR-VA-TR-2012-0011

12. DISTRIBUTION/AVAILABILITY STATEMENT
Unclassified

13. SUPPLEMENTARY NOTES

14. ABSTRACT

Nanotoxicology: An emerging discipline evolving from studies of ultrafine particles.

Although humans have been exposed to airborne nanosized particles (NSPs; < 100 nm) throughout their evolutionary stages, such exposure has increased dramatically over the last century due to anthropogenic sources. The rapidly developing field of nanotechnology is likely to become yet another source through inhalation, ingestion, skin uptake, and injection of engineered nanomaterials. Information about safety and potential hazards is urgently needed. Results of older biokinetic studies with NSPs and newer epidemiologic and toxicologic studies with airborne ultrafine particles can be viewed as the basis for the expanding field of nanotoxicology, which can be defined as safety evaluation of engineered nanostructures and nanodevices. Collectively, some emerging concepts of nanotoxicology can be identified from the results of these studies. When inhaled, specific sizes of NSPs are efficiently deposited by diffusional mechanisms in all regions of the respiratory tract. The small size facilitates uptake into cells and transcytosis across epithelial and endothelial cells into the blood and lymph circulation to reach potentially sensitive target site

15. SUBJECT TERMS

16. SECURITY CLASSIFICATION OF:			17. LIMITATION OF ABSTRACT	18. NUMBER OF PAGES	19a. NAME OF RESPONSIBLE PERSON
a. REPORT	b. ABSTRACT	c. THIS PAGE			Günter Oberdörster
U	U	U	UU	44	19b. TELEPHONE NUMBER *(Include area code)* 585-275-3804

ROCHESTER MURI PROJECT – FINAL REPORT

January, 2012

Title of Proposal: *Correlation Between Physicochemical Characteristics and Toxicological Properties of Nanomaterials*

Award Number: FA9550-04-1-0430

Name of Institution: University of Rochester

Authors of Report:

Günter Oberdörster (gunter_oberdorster@urmc.rochester.edu)
University of Rochester
Department of Environmental Medicine
575 Elmwood Avenue, Medical Center Box 850
Rochester, NY 14642
Tele: 585-275-3804/fax: 585-256-2631

David Pui (dyhpui@tc.umn.edu)
University of Minnesota
Mechanical Engineering
111 Church St SE
Minneapolis, MN 55455
Tele: 612-625-2537

Pratim Biswas (pratim.biswas@seas.wustl.edu)
Department of Chemical Engineering
Washington University in St. Louis
One Brookings Drive, Campus Box 1180
St. Louis, MO 63130
Tele: 314-935-5482 (5548)

(For additional authors - see individual writeups)

Publications [2005-present] (copies have been submitted to AFOSR):

Biswas, P. and Wu, C-Y. Nanoparticles and the environment. J. Air & Waste Management Assoc. 55: 708-746, 2005.

Braydich-Stolle, Schaeublin, Murdock, Jiang, Biswas, Schlager, and Hussain. "Crystal Structure Mediates Mode of Death in TiO_2 Nanotoxicity". *J. Nanopart. Res*. (2009) 11: 1361-1374.

Cho and Biswas, Sintering Rates for Pristine and Doped Titanium Dioxide Determined Using a Tandem Differential Mobility Analyzer System; Aerosol Science and Technology, 40:309-319, 2006

Cho and Biswas, A geometrical sintering model (GSM) to predict surface area change; J. Aerosol Sci., 37: 1378-1387, 2006.

Ehrenberg, M. and McGrath, J.L. Binding between particles and proteins in extracts: implications for microrheology and toxicity. Acta Biomaterialia 1: 305-315, 2005.

Ehrenberg MS, Friedman AE, Finkelstein JN, Oberdörster G, McGrath JL. The influence of protein adsorption on nanoparticle association with cultured endothelial cells. Biomaterials 30: 603-610, 2009.

Elder A, Gelein R, Silva V, Feikert T, Opanashuk L, Carter J, Potter R, Maynard A, Ito Y, Finkelstein J, Oberdörster G. Translocation of inhaled ultrafine manganese oxide particles to the central nervous system. Environ. Health Perspect Environ. Health Perspect. 114(8): 1172-1178, 2006. (doi: 10.1289/ehp.9030 [available at http://dx.doi.org/), on-line 20 April 2006.

Elder A, Yang, H, Gwiazda R, Teng X, Thurston S, He H, Oberdörster G. Testing nanomaterials of unkown toxicity: An example based on Platinum nanoparticles of different shapes. Advanced Materials, 19: 3124-3129, 2007.

C. M. Evans, L. Guo, J. J. Peterson, S. Maccagnano, and T. D. Krauss, "Ultra-bright PbSe Magic Sized Clusters," *Nano Lett.* **8**, 2896-2899, 2008 (web release 8/1/08).

Gaborski, T. R., M. N. Sealander, M. S. Ehrenberg, R. E. Waugh and McGrath, J.L., 2010. Image Correlation Microscopy for Uniform Illumination J. Microscopy 237, 39-50

M. A. Hahn, P. C. Keng, and T. D. Krauss, "Flow Cytometric Analysis to Detect Pathogens in Bacterial Cell Mixtures using Semiconductor Quantum Dots," *Anal. Chem,* **80**, 864-872 (2008).

Han X, Gelein R, Corson N, et al. (2011). Validation of an LDH assay for assessing nanoparticle toxicity. Toxicology 287: 99-104

Hogan, Kettleson, Ramaswami, Chen, and Biswas. Charge Reduced Electrospray Size Spectrometry of Mega- and Gigadalton Complexes: Whole Viruses and Virus Fragments; Anal. Chem. 2006, 78,844-852

Huang, L.-S. and Chen, J. (2008) Analysis of variance, regression. Annals of Statistics36 (No. 5): 2085-2109.

Huang, L.-S. and Su, H. (2008) Nonparametric F-tests for nested global and local polynomial models. J. Stat. Planning and Inference, doi: 10.1016/j.jspi.2008.08.013.

Jiang, Lee and Biswas, J. Model for Nanoparticle Charging by Diffusion, Direct Photoionization, and Thermionization Mechanisms; J. of Electrostatics 65: 209-220, 2007.

Jiang, J., Hogan, C.J., Chen, D.R., Biswas, P., "Aerosol charging and capture in the nanoparticle size range (6-15 nm) by direct photoionization and diffusion mechanisms", *Journal of Applied Physics*, 102, 034904 (2007).

Jiang J., Chen D. R., Biswas P. "Synthesis of Nanoparticles in a Flame Aerosol Reactor with Independent and Strict Control of their Size, Crystal Phase, and Morphology", *Nanotechnology*, 18, 285603, 2007.

Jiang, J, Oberdörster G, Elder, A, Gelein R, Mercer P, Biswas P. Does nanoparticle activity depend upon size and crystal phase? Nanotoxicology 2 (1): 33-42, March, 2008.

Jiang, J., Oberdörster, G., Biswas, P. Characterization of size, surface charge, and agglomeration state of nanoparticle dispersions for toxicological studies. J Nanopart. Res. (on-line June, 2008), 11:77-89, 2009.

Kim, SC, Chen, D-R, Qi, C., Gelein RM, Finkelstein, JN, Elder A, Bentley K, Oberdörster G, and Pui DYH. A nanoparticle dispersion method for in vitro and in vivo nanotoxicity study. Nanotoxicology 4(1), 42-51, 2010.

Kreyling, W.G., Möller, W., Schmid, O., Semmler-Behnke, M., Oberdörster, G. In: Cardiovascular Effects of Inhaled Ultrafine and Nano-sized Particles. Chapter 7: Translocation of Inhaled Nanoparticles. pgs. 125-143, edited by: Cassee, Mils and Newby, John Wiley & Sons, Inc. Publication, 2011.

Lynch, I., A. Elder. Disposition of Nanoparticles as a Function of their Interactions with Biomolecules. In Nanotechnology: Risks and Benefits, I. Linkov and J. Steevens (eds.). Dordrecht: Springer, 11 pp., 2009.

Maksimuk, S., Teng, X., Yang, H. Planar tripods of platinum: formation and self-assembly, 2006, Phys. Chem. Chem. Phys. 8: 4660-4663, DOI 10.1039/b611186f.

Mortensen, LJ, Oberdörster, G, Pentland, AP, DeLouise, LA. (2008). *In vivo* skin penetration of quantum dot nanopartiles in the murine model: The effect of UVR. Nano Letters; available at: http://pubs.acs.org/journals/nalefd/index.html (8/2008 - web release 8/8/08).

Oberdörster, G., Oberdörster, E. and Oberdörster, J. Nanotoxicology: An emerging discipline evolving from studies of ultrafine particles. Environmental Health Perspectives 113, No. 7: 823-839, 2005.

Oberdörster, G., Stone, V., Donaldson, K. Toxicology of nanoparticles: A historical perspective. Nanotoxicology, March, 2007; 1(1): 2-25.

Oberdörster, G. Biokinetics and effects of nanoparticles. In: Nanotechnology – Toxicological Issues and Environmental Safety, pgs. 15-51, 2007. Edited by: P.P. Simeonova, N. Opopol, M. I. Luster. NATO Science for Peace and Security Series – C: Environmental Security, Springer Publishers with NATO Public Diplomacy Division.

Oberdörster, G., Elder, A., Rinderknecht, A. Nanoparticles and the Brain: Cause for Concern? J. Nanoscience and Nanotechnology 9 (No. 8): 4996-5007, 2009.

Oberdörster, G. Safety assessment for nanotechnology and nanomedicine: concepts of nanotoxicology. J. Internal Medicine 267: 89-105, 2009.

Rushton, EK, Jiang, J, Leonard SS, Eberly S, Castranova V, Biswas P, Elder A, Han X, Gelein R, Finkelstein J, Oberdörster G. Concept of assessing nanoparticle hazards considering nanoparticle dosemetric and chemical/biological response-metrics. JTEH, Part A, 73: 445-461, 2010.

Sahu, M. and P. Biswas, Concentration and Size Distribution of Nanoparticles in a Research Laboratory Working Environment with Nanomaterial Synthesis Reactors. Journal of Nanoparticle Research, 12 (3), 1055-1064, 2010

Semmler-Behnke, M., Takenaka, S., Fertsch, S., Wenk, A., Seitz, J., Mayer, P., Oberdörster, G., Kreyling, W.G. Efficient elimination of inhaled nanoparticles from the alveolar region: evidence for interstitial uptake and subsequent re-entrainment onto airways epithelia. Environ. Health Perspectives, on-line 6 February 2007 (doi: 10.1289/ehp.9685 [available at: http://dx.doi.org/]); 115: 728-733, May, 2007.

Suttiponparnit, K., J. Jiang, M. Sahu, S. Suvachittanont, T. Charinpanitku, and P. Biswas, Role of Surface area, Primary Particle size, and Crystal Phase on Titanium Dioxide Nanoparticle Dispersion Properties, Nanoscale Research Letters, 2010 (Accepted, 8/2010).

Teng, X. and Yang, H. Synthesis of platinum multipods: an induced anisotropic growth. NanoLetters5: 885-891, 2005.

VanWinkle, BA, de Mesy Bentley, KL, Malecki, JM, Gunter, KK, Evans IM, Elder A, Finkelstein JN, Oberdörster G, Gunter, TE. 2009. Nanoparticle (NP) uptake by type I alveolar epithelial cells and their oxidant stress response. Nanotoxicology1-12, iFirstarticle.

Wu, B, R. Huang, M. Sahu, X. Feng, P. Biswas, and Y.J. Tang, Bacterial Responses to Cu-doped TiO2 Nanoparticles, Science of the Total Environment, 408 (7), 1755-1758, 2010.

Yang, H. and Xia, Y. Bionanotechnology: Enabling biomedical research with nanomaterials. Adv. Mater. 19: 3085-3087, 2007.

Z. Yu, M. Hahn, J. Calcines, T. D. Krauss, E. Alldredge, and J. Silcox, "Small-angle Rotation in Individual Colloidal CdSe Quantum Rods," ACS Nano 2, 1179-1188 (2008).

Book Chapters:

DeLouise, L.A., Mortensen, L.; Elder, A., "Breeching Epithelial Barriers - Physiochemical Factors Impacting Nanoparticle Translocation and Toxicity", in "Safety of Nanoparticles: From Manufacturing to Clinical Applications" Ed. Tom Webster, Springer.

Lynch, I., A. Elder. Disposition of Nanoparticles as a Function of their Interactions with Biomolecules. In Nanotechnology: Risks and Benefits, I. Linkov and J. Steevens (eds.). Dordrecht: Springer, 11 pp., 2009.

Upadhyay, S., **A. Elder**, W.E. Cascio, H. Schulz. Particles and the autonomic nervous system. In *Particles and Cardiovascular Disease Mechanisms*, Eds. F.R. Cassee, N.L. Mills, D.E. Newby. John Wiley & Sons, Inc., Hoboken, NJ. In press.

Elder, A., I. Lynch, K. Grieger, S. Chan-Remillard, A. Gatti, H. Gnewuch, E. Kenawy, R. Korenstein, T. Kuhlbusch, F. Linker, S. Matias, N. Monteiro-Riviere, V. Pinto, R. Rudnitsky, K. Savoleinen, A. Shvedova. Human Health Risks of Engineered Nanomaterials. In *Nanotechnology: Risks and Benefits*, I. Linkov and J. Steevens (eds.). Dordrecht: Springer, 27 pp., 2009.

UNIVERSITY OF ROCHESTER

Günter Oberdörster (gunter_oberdorster@urmc.rochester.edu)
Alison Elder (alison_elder@urmc.rochester.edu)
Jacob Finkelstein (jacob_finkelstein@urmc.rochester.edu)
Thomas Gunter (thomas_gunter@urmc.rochester.edu)
Jim McGrath (jim_mcgrath@urmc.rocheser.edu)
Todd Krauss (krauss@chem.rochester.edu)
Lisa DeLouise (lisa_delouise@urmc.rochester.edu)

Postdoctoral Fellows:
Amber Rinderknecht (amber_rinderknecht@urmc.rochester.edu)
Zhihui Ban

Students:
Mort Ehrenberg
Xianglu Han
Megan Hahn
Luke Mortensen
Beth Van Winkle
Li Guo
Helen Wei
Kathryn Leach

Research Summaries:

Nanotoxicology: An emerging discipline evolving from studies of ultrafine particles.

Although humans have been exposed to airborne nanosized particles (NSPs; < 100 nm) throughout their evolutionary stages, such exposure has increased dramatically over the last century due to anthropogenic sources. The rapidly developing field of nanotechnology is likely to become yet another source through inhalation, ingestion, skin uptake, and injection of engineered nanomaterials. Information about safety and potential hazards is urgently needed. Results of older biokinetic studies with NSPs and newer epidemiologic and toxicologic studies with airborne ultrafine particles can be viewed as the basis for the expanding field of nanotoxicology, which can be defined as safety evaluation of engineered nanostructures and nanodevices. Collectively, some emerging concepts of nanotoxicology can be identified from the results of these studies. When inhaled, specific sizes of NSPs are efficiently deposited by diffusional mechanisms in all regions of the respiratory tract. The small size facilitates uptake into cells and transcytosis across epithelial and endothelial cells into the blood and lymph circulation to reach potentially sensitive target sites such as bone marrow, lymph nodes, spleen, and heart. Access to the central nervous system and ganglia via translocation along axons and dendrites of neurons has also been observed. NSPs penetrating the skin distribute via uptake into lymphatic channels. Endocytosis and biokinetics are largely dependent on NSP surface chemistry (coating) and in vivo surface modifications. The greater surface area per mass compared with larger-sized particles of the same chemistry renders NSPs more active biologically. This activity includes a potential for inflammatory and pro-oxidant, but also antioxidant, activity, which can explain early findings showing mixed results in terms of toxicity of NSPs to environmentally relevant species. Evidence of mitochondrial distribution and oxidative stress response after NSP endocytosis points to a need for basic research on their interactions with subcellular structures. Additional considerations for assessing safety of engineered NSPs include careful selections of appropriate and relevant doses/concentrations, the likelihood of increased effects in a compromised organism, and also the benefits of possible desirable effects. An interdisciplinary team approach (e.g., toxicology, materials science, medicine, molecular biology, and bioinformatics, to name a few) is mandatory for nanotoxicology research to arrive at an appropriate risk assessment.

Translocation of inhaled ultrafine manganese oxide particles to the central nervous system.

Background: Studies in monkeys with intranasally instilled gold ultrafine particles (UFP, <100 nm) and in rats with inhaled carbon UFP suggested that solid UFP deposited in the nose travel along the olfactory nerve to the olfactory bulb. Methods: To determine if olfactory translocation occurs for other solid metal UFP and assess potential health effects, we exposed groups of rats to Mn oxide UFP (30 nm; ~500 **μ**g/m3) with either both nostrils patent or the right nostril occluded. Analyses of Mn in lung, liver, olfactory bulb, and other brain regions were performed, as well as gene and protein analyses. Results: After 12 days of exposure with both nostrils patent, Mn concentrations in the olfactory bulb increased 3.5-fold, whereas lung Mn concentrations doubled; there were also increases in striatum, frontal cortex, and cerebellum. Lung lavage analysis showed no indications of lung inflammation, whereas increases in olfactory bulb TNF-**α** mRNA (~8-fold) and protein (~30-fold) were found after 11 days of exposure and, to a lesser degree, in other brain regions with increased Mn levels. MIP-2, GFAP, and NCAM mRNA were also increased in olfactory bulb. With the right nostril occluded for a 2-day exposure, Mn accumulated only in the left olfactory bulb. Solubilization of the Mn oxide UFP was ~1.5% per day. Conclusions: We conclude that the olfactory neuronal pathway is efficient for translocating inhaled Mn oxide as solid UFP to the CNS and that this can result in inflammatory changes. We suggest that despite differences between human and rodent olfactory systems, this pathway is relevant in humans.

Nanoparticle (NP) uptake by type I alveolar epithelial cells and their oxidant stress response.

Mammalian cells take up nanoparticles and some nanoparticles increase reactive oxygen species (ROS). Characteristics of ROS producing nanoparticles and whether ROS production correlates with cell exposure/uptake are active areas of investigation. We have documented uptake with images and measured ROS in parallel to evaluate nanoparticle-cell interactions. This visualization study focuses on type I-like cells, called R3-1 cells, exposed to nanoparticles at 1.2 **μ**g/cm^2 ([~4-6**μ**g/ml]) in media. Titanium dioxide (Ti02), gold (Au), silver (Ag), and manganese (Mn) were internalized, copper (Cu) particles were not but were observed at the cell surface at short exposure times. TiO_2 and Au did not increase cell death after several days. Mn nanoparticles increased cell death over 72 hours. Cu nanoparticles caused 50% cell death in 24 hours, the surviving cells recovered and proliferated. Ag nanoparticles caused 80% of the cells to lift off the slides within one hour. Amplex Red was used to report H_2O_2 production after cell exposure to 0.4 **μ**g/cm^2; [~1**μ**g/ml] TiO_2, Au, Cu, Mn and Ag. TiO_2, Au, and Ag caused no significant increase in H_2O_2, while Cu and Mn greatly increase H_2O_2. Nanoparticles give up electrons during oxidation increase ROS production and cell death in R3-1 cells.

Toxicology of nanoparticles: A historical perspective.

The rapid expansion of nanotechnology promises to have great benefits for society, yet there is increasing concern that human and environmental exposure to engineered nanomaterials may result in significant adverse effects. That is why the field of nanotoxicology – dealing with effects and potential risks of particulate structures <100 nm in size – has emerged, growing significantly over the past decade from long-standing foundations of well established knowledge on the toxicology of fibrous and non-fibrous particles and the interactions of viruses with cells. This review places nanoparticles in the context of conventional particle toxicology and so includes references to other types of particles, such as silica and asbestos, which have been extensively studied and can provide useful lessons relevant to newly engineered nanoparticles (NP). Discoveries of nanoparticle-specific concepts of toxicology related to their small size and large specific surface area go back to the early parts of the past century, although the distinctive biological effects and kinetics of NP were not recognized until the last decade of the past century. Today, the propensity of NP to cross cell barriers, enter cells and interact with subcellular structures is well established, as is the induction of oxidative stress as a major mechanism of nanoparticle effects. In addition to the significance of small size and surface area of NP, uncovering the impact of many other physico-chemical characteristics – in particular NP surface properties – for initiating effects in the mammalian organism and the environment is now an active area of research. The article aims to cover hazards relevant to humans, provides an introduction to some of the newly emerging literature on fate and behavior of NP in the environment, as wellas describing their ecotoxicology in a variety of species. Major milestones in the research leading to our present understanding of nanotoxicology and the potential risks of NP to humans and the environment are summarized. These risks are likely to be different for different nanomaterials, ranging from perceived and very low for most, to real and very high for some. There are many questions

that remain to be addressed, and we foresee for the future a continuing extended research in nanotoxicology. A full understanding of the hazard of NP will make a major contribution to the risk assessment that is so urgently needed to ensure that products that utilize NP are made safely, are exploited to their full potential and then disposed of safely.

In vivo skin penetration of quantum dot nanopartiles in the murine model: The effect of UVR.

Ultraviolet radiation (UVR) has widespread effects on the biology and integrity of the skin barrier. Research on the mechanisms that drive these changes, as well as their effect on skin barrier function, has been ongoing since the 1980s. However, no studies have examined the impact of UVR on nanoparticle skin penetration. Nanoparticles (NP) are commonly used in sunscreens and other cosmetics, and since consumer use of sunscreen is often applied to sun damaged skin, the effect of UVR on NP skin penetration is a concern due to potential toxicity. In this study, we investigate NP skin penetration by employing an in vivo semiconductor quantum dot nanoparticle (QD) model system. This model system improves NP imaging capabilities and provides additional primary interest due to widespread and expanding use of QD in research applications and manufacturing. In our experiments, carboxylated QD were applied to the skin of SKH-1 mice in a glycerol vehicle with and without UVR exposure. The skin collection and penetration patterns were evaluated 8 and 24 h after QD application using tissue histology, confocal microscopy, and transmission electron microscopy (TEM) with EDAX analysis. Low levels of penetration were seen in both the non-UVR exposed mice and the UVR exposed mice. Qualitatively higher levels of penetration were observable in the UVR exposed mice. These results are the first for in vivo QD skin penetration, and provide important insight into the ability of QD to penetrate intact and UVR compromised skin barrier. Our findings raise concern that NP of similar size and surface chemistry, such as metal oxide NP found in sunscreens, may also penetrate UV damaged skin.

Testing nanomaterials of unkown toxicity: An example based on Platinum nanoparticles of different shapes.

Manipulation of the physicochemical properties of materials at the nanoscale has the potential to significantly improve their electronic, diagnostic, and therapeutic performance. Because of the intended use of nanomaterials and the potential for accidental exposures, it is important to determine if there is any unique toxicity of the nanoscale materials as compared to the bulk. A likely portal of entry following accidental exposure is the lung. As has been demonstrated for nanosized ambient air-borne particles that are largely insoluble,[1-4] engineered nanoparticles (NPs) may also evade macrophage-mediated particle clearance mechanisms at the site of deposition in the lungs, potentially coming into contact with epithelial and endothelial cells and translocating to distant sites. Inflammation and oxidant stress responses may occur as a result of prolonged retention and unique physicochemical properties of the NPs. It is thought that NPs, either on their own or when combined with cells, produce oxidant species that cause injury to and antioxidant depletion in cells or tissues.[5-7] The same properties that can be manipulated to produce unique characteristics at the nanoscale, such as size, shape, composition, crystal phase, and surface coatings, may also impart toxicity that is not observed with larger particles or bulk samples.

Nanoparticles and the Brain: Cause for Concern?

Engineered nanoparticles (NPs) are in the same size category as atmospheric ultrafine particles, <100 nm. Per given volume, both have high numbers and surface areas compared to larger particles. The high proportion of surface atoms/molecules can give rise to a greater chemical as well as biological activity, for example the induction of reactive oxygen species in cell-free medium as well as in cells. When inhaled as singlet particles, NPs of different sizes deposit efficiently in all regions of the respiratory tract by diffusion. A major difference to larger size particles is the propensity of NPs to translocate across cell barriers from the portal of entry (e.g., the respiratory tract) to secondary organs and to enter cells by various mechanisms and associate with subcellular structures. This makes NPs uniquely suitable for therapeutic and diagnostic uses, but it also leaves target organs such as the central nervous system (CNS) vulnerable to potential adverse effects (e.g., oxidative stress). Neuronal transport of NPs has been described, involving retrograde and anterograde movement in axons and dendrites as well as perineural translocation. This is of importance for access of inhaled NPs to the CNS via sensory nerves existing in the nasopharyngeal and tracheobronchial regions of the respiratory tract. The neuronal pathway circumvents the very tight blood brain barrier. In general, translocation rates of NP from the portal of entry into the blood compartment or

the CNS are very low. Important modifiers of translocation are the physicochemical characteristics of NPs, most notably their size and surface properties, particularly surface chemistry. Primary surface coating (when NPs are manufactured) and secondary surface coating (adsorption of lipids/proteins occurring at the portal of entry and during subsequent translocation) can significantly alter NP biokinetics and their effects. Implications of species differences in respiratory tract anatomy, breathing pattern and brain anatomy for extrapolation to humans of NP effects observed in rodents need to be considered. Although there are anecdotal data indicating a causal relationship between long-term ultrafine particle exposures in ambient air (e.g., traffic related) or at the workplace (e.g., metal fumes) and resultant neurotoxic effects in humans, more studies are needed to test the hypothesis that inhaled nanoparticles cause neurodegenerative effects. Some but probably not the majority of NPs will have a significant toxicity (hazard) potential, and this will pose a significant risk if there is a sufficient exposure. The challenge is to identify such hazardous NPs and take appropriate measures to prevent exposure.

Concept of assessing nanoparticle hazards considering nano-particle dosemetric and chemical/biological response-metrics

Engineered nanoparticles (NP) are being developed and incorporated in a number of commercial products, raising the potential of human exposure during manufacture, use, and disposal. Although data concerning the potential toxicity of some NP have been reported, validated simple assays are lacking for predicting their in vivo toxicity. The aim of this study was to evaluate new response metrics based on chemical and biological activity of NP for screening assays that can be used to predict NP toxicity in vivo. Two cell-free and two cell-based assays were evaluated for their power in predicting in vivo toxicity of eight distinct particle types with widely differing physicochemical characteristics. The cell-free systems comprised fluorescence- and electron spin resonance-based assays of oxidant activity. The cell-based systems also used electron spin resonance (ESR) as well as luciferase reporter activity to rank the different particle types in comparison to benchmark particles of low and high activity. In vivo experiments evaluated acute pulmonary inflammatory responses in rats. Endpoints in all assays were related to oxidative stress and responses were expressed per unit NP surface area to compare the results of different assays. Results indicated that NP are capable of producing reactive species, which in biological systems lead to oxidative stress. Copper NP had the greatest activity in all assays, while TiO_2 and gold NP generally were the least reactive. Differences in the ranking of NP activity among the assays were found when comparisons were based on measured responses. However, expressing the chemical (cell-free) and biological (cells; in vivo) activity per unit particle surface area showed that all in vitro assays correlated significantly with in vivo results, with the cellular assays correlating the best. Data from this study indicate that it is possible to predict acute in vivo inflammatory potential of NP with cell-free and cellular assays by using NP surface area-based dose and response metrics, but that a cellular component is required to achieve a higher degree of predictive power.

Validation of an LDH assay for assessing nanoparticle toxicity

Studies showed that certain cytotoxicity assays were not suitable for assessing nanoparticle (NP) toxicity. We evaluated a lactate dehydrogenase (LDH) assay for assessing copper (Cu-40, 40 nm), silver (Ag-35, 35 nm; Ag-40, 40 nm), and titanium dioxide (TiO_2-25, 25 nm) NPs by examining their potential to inactivate LDH and interference with β-nicotinamide adenine dinucleotide (NADH), a substrate for the assay. We also performed a dissolution assay for some of the NPs. We found that the copper NPs, because of their high dissolution rate, could interfere with the LDH assay by inactivating LDH. Ag-35 could also inactivate LDH probably because of the carbon matrix used to cage the particles during synthesis. TiO_2-25 NPs were found to adsorb LDH molecules. In conclusion, NP interference with the LDH assay depends on the type of NPs and the suitability of the assay for assessing NP toxicity should be examined case by case.

Safety assessment for nanotechnology and nanomedicine: concepts of nanotoxicology.

Nanotechnology, nanomedicine and nanotoxicology are complementary disciplines aimed at the betterment of human life. However, concerns have been expressed about risks posed by engineered nanomaterials (ENMs), their potential to cause undesirable effects, contaminate the environment and adversely affect susceptible parts of the population. Information about toxicity and biokinetics of nano-enabled products combined with the knowledge of unintentional human and environmental exposure or intentional delivery for medicinal purposes will be necessary to determine real or perceived risks of

nanomaterials. Yet, results of toxicological studies using only extraordinarily high experimental doses have to be interpreted with caution. Key concepts of nanotoxicology are addressed, including significance of dose, dose rate, and biokinetics, which are exemplified by specific findings of ENM toxicity, and by discussing the importance of detailed physicochemical characterization of nanoparticles, specifically surface properties. Thorough evaluation of desirable versus adverse effects is required for safe applications of ENMs, and major challenges lie ahead to answer key questions of nanotoxicology. Foremost are assessment of human and environmental exposure, and biokinetics or pharmacokinetics, identification of potential hazards, and biopersistence in cells and subcellular structures to perform meaningful risk assessments. A specific example of multiwalled carbon nanotubes (MWCNT) illustrates the difficulty of extrapolating toxicological results. MWCNT were found to cause asbestos-like effects of the mesothelium following intracavitary injection of high doses in rodents. The important question of whether inhaled MWCNT will translocate to sensitive mesothelial sites has not been answered yet. Even without being able to perform a quantitative risk assessment for ENMs, due to the lack of sufficient data on exposure, biokinetics and organ toxicity, until we know better it should be made mandatory to prevent exposure by appropriate precautionary measures / regulations and practicing best industrial hygiene to avoid future horror scenarios from environmental or occupational exposures. Similarly, safety assessment for medical applications as key contribution of nanotoxicology to nanomedicine relies heavily on nano-specific toxicological concepts and findings and on a multidisciplinary collaborative approach involving material scientists, physicians and toxicologists.

Jim McGrath (jim_mcgrath@urmc.rochester.edu)
University of Rochester
Biomedical Engineering

Findings and Accomplishments:

Ehrenberg, M. and McGrath, J.L. 2005 Binding between particles and proteins in extracts: implications for microrheology and toxicity. Acta Biomaterialia, 1:305-315.
Here we characterized the natural capacity of various particles to bind to the proteins contained in fibroblast cytoplasm and bovine brain extracts. We found that all particles tested (polystyrene, TiO_2, and SiO_2 with various levels of surface carboxylation) bound primarily to cytoskeletal proteins in both extracts, although the profile of bound proteins did vary with particle surface chemistry and extract type. In the fibroblast extracts, we found that carboxylated polystyrene beads bind most prominantly to actin and the intermediate filament protein vimentin, and through surface modification we could eliminate the binding of actin. These biochemical studies were supported with microrheological measurements in living fibroblast cytoplasm. Here we tracked particles with high temporal and spatial resolution and found that the untreated particles made random movements of diminished amplitude compared to the particles treated to block actin binding.

Ehrenberg, M.S., Friedman, A.E., Finkelstein, J.N., Oberdörster, G., and McGrath, J.L. 2009, The influence of protein adsorption on nanoparticle association with cultured endothelial cells. Biomaterials 30, 603-610.

Because nanoparticles (NP) will typically travel through biological fluids before they reach cellular surfaces, we sought to understand the impact of surface absorption of proteins from protein-rich solutions on the interaction of NPs with cells. As a model system, we choose to study human umbilical vein endothelial cells (HUVEC) and nanoparticles exposed to serum components. This is an established, well-characterized culture system and a reasonable model for NP transport to tissue via blood. We used ~100 nm polystyrene particles because these are readily available as fluorescent particles with different surface chemistries. The following are the primary methods and findings of this work.

(a) Our first studies showed that proteins stably coat NPs after a10 minute exposure to serum and that the protein coat determines both NP surface charge (zeta potential) and size. Because NP binding to cells occurs on times scales of hours to days, these results indicate that adsorbed proteins are important to understanding the NP surface chemistry presented to cells.
(b) We developed a quantitative FACS-based assay for measuring the number of particles associated with endothelial cells. Combining this technique with measures of protein absorption to NPs we report a correlation between the capacity of NPs to bind protein and their tendency to associate with cells.
(c) To determine if particular proteins from serum were responsible for driving NP association with cells, we used a state-of-the-art affinity-based depletion process to remove the 12 most abundant proteins from serum. The levels and kinetics of

cell association for particles incubated in complete vs. depleted serum was unchanged and switching species of serum from human to bovine also did not affect association. This data suggests that the binding of NPs to endothelial cells is largely driven by non-specific interactions rather than particular ligand-receptor interactions.

Gaborski, T. R., M. N. Sealander, M. S. Ehrenberg, R. E. Waugh and McGrath, J.L., 2010 Image Correlation Microscopy for Uniform Illumination J. Microscopy 237, 39-50

This paper develops techniques for determining the mobility of a field of nanoparticles using image correlation. The paper validates the method against the single particle tracking techniques in Ehrenberg et al. (2005). The technique is a rapid way of obtaining average motility date for a system of nanoparticles internalized in a cell or tissue.

Ehrenberg, M. and McGrath, J.L. Nanoparticle clustering in endothelial cells. In preparation for Acta Biomaterialia

As a follow up to our first MURI-sponsored work (Ehrenberg, M. and McGrath, J.L. 2005 Acta Biomaterialia, 1:305-315) we examined the intracellular motions of NPs that were placed directly into cell cytoplasm through microinjection vs. those that placed in media and entered cells through natural endocytic pathways. Here we looked more carefully at the fate of nanoparticles that were endocytosed and the role of particle surface chemistry. The following are the primary methods and findings of this work.

- We found that ~100nm polystyrene particles with amine, amidine and carboxlate surfaces were endocytosed by endothelial cells and that their distribution within cells progressed from an approximately uniform distribution to a strongly perinuclear distribution over the course of several days. The results suggest that new particles enter the cell over much of the plasma membrane but steadily traffic to perinuclear stores where they accumulate.
- Internal membrane labels revealed that most nanoparticles were in lysosomes. We also examined the effects of pH on protein binding to NPs and found that the acidic pHs in lysosomes produced significantly more protein binding to NPs than neutral or basic pHs. These results held for all three particle types.
- In addition to image processing algortihms that determined the position of nanoparticles relative to nucleii, we developed methods for quantifying the size of NP clusters and the number of NPs in a cluster. Our results show that NPs all aggregate as they localize in endosomes but to degrees that depend on NP surface chemistry. Given higher protein binding at acidic pH, the clustering is likely driven by denatured proteins in lysosomes that can cross-link NPs into aggregates.
- Cytoskeletal poisons that disrupt either actin and microtubules tend to keep nanoparticles more uniformly distributed in cell cytoplasm, although perinuclear accumulation still occurs. The data are most striking for microtuble disruption suggesting some influence of microtubule in trafficking vesicles contianing NPs toward perinuclear stores.

Theses:

Morton Ehrenberg, PhD *The Physiochemical basis of nanoparticle interactions with cells: application and analysis.*

Available for electronic download at: https://urresearch.rochester.edu

Dr. Ehrenberg's thesis was directly supported by the MURI project. His contributions are summarized in two published papers and one unpublished paper described below.

Thomas Gaborski, PhD *Quantitative methods for understanding physical mechanisms of neutrophil adhesion*

Available for electronic download at: https://urresearch.rochester.edu

Dr. Gaborski' thesis was not directly supported by the MURI project however one of his studies, Gaborski et al. (2010) J. Microscopy 237: 39-50, developed methods for determining the mobility of fields nanoparticles and used a low-light camera (Cooke Sensicam) originally purchased with MURI funds.

Related Presentations:

McGrath, JL, "Nanoparticle surface properties control interactions with cytoskeleton," Society of Toxicity," Seattle, WA March 2008

McGrath, JL and Ehrenberg, M. "Nanoparticle interactions with the cytoskeleton" Particles 2006: Medical/Biochemical Diagnostic, Pharmaceutical, and Drug Delivery Applications of Particle Technology, Orlando, May 2006

Ehrenberg, M. and McGrath, JL "Particle interactions with cytoskeleton," 2nd International Symposium on Nanotechnology and Occupational Health, Minneapolis, MN, October 2005

Thomas E. Gunter (thomas_gunter@urmc.rochester.edu)
University of Rochester
Department of Biochemistry

Production of reactive oxygen species by metal/metal oxide nanoparticles and their effects leading to cell death in a type I alveolar cell model.

For the last several years we have worked on showing the relationship between the production of reactive oxygen species (ROS) and cell damage and death produced by nanoparticles. We have focused both on ROS produced by the mitochondrial electron transport chain and on ROS produced by other sources following exposure of type 1 alveolar epithelial cells (R3-1 cells) to metal and metal oxide nanoparticles in the size range from 20 to 60 nm. The nanoparticles studied were TiO_2, Au, Ag, and Cu nanoparticles from commercial sources and Mn/Mn oxide nanoparticles made by an electric arch discharge in a Palas generator. Most of the work in the last year has involved completing the work on the Cu and Ag nanoparticles.

The results have shown that all of these nanoparticles except the Cu nanoparticles get inside the cells rapidly over a period of minutes to hours as determined by electron microscopy (TEM) and elemental analysis (EDS). The reason that few if any Cu nanoparticles are seen inside cells seems related to the rapid disappearance of these particles through dissolving in the cell medium. TiO_2, Au, and Mn nanoparticles are found in the cell cytosol, lysosomes, and occasionally inside the mitochondria. Ag nanoparticles get into the cell most rapidly of all those nanoparticles studied and are found throughout the cell including the nucleus. There is some evidence that they enter the nucleus through nuclear pores. While there is some evidence that ROS production by mitochondria is stimulated by the Mn nanoparticles, there is clearly a much larger production of ROS by reduction reactions caused by the Mn and Cu nanoparticles themselves. Little or no increase in ROS production was seen after uptake of TiO_2, Au, and Ag nanoparticles, but a large increase in ROS production was seen in the presence of Mn and Cu nanoparticles. Both of these types of nanoparticles were mixtures of metal and metal oxides and there is evidence that the ROS formed was primarily H_2O_2 formed through a reaction of the type $Me(s) + O_2 + 2H^+ = Me^{2+} + H_2O_2$. The Cu nanoparticles rapidly damaged the cell exterior while the Mn nanoparticles primarily caused damage to the microsomes leading to heteromicrosomes. Both induced cell death.

This work has now been published as: Nanoparticle (NP) uptake by type I alveolar epithelial cells and their oxidant stress response by B. A. Van Winkle, K. de M. Bentley, J. M. Malecki, K. K. Gunter, I. M. Evans, A. Elder, J. N. Finkelstein, G. Oberdorster, and T. E. Gunter in Nanotoxicology DOI 10.1080/17435390903121949, (2009).

Todd D. Krauss
Department of Chemistry
University of Rochester
krauss@chem.rochester.edu

Key Findings During Course of Program

Au Nanoparticle Functionalization

When investigating the toxicological effects of nanoparticles, one has to consider the material comprising the particle, the particle size and shape, and the particle surface coating. We decided to focus a significant effort on colloidal Au nanoparticles, since the nanoparticle material and the particle size and shape would be well defined. In addition, for Au nanoparticles this well-defined particle size is easily tuned and the surface functionality can be easily modified.

We initially developed a protocol for conjugating the protein albumin to the surface of Au nanoparticles to acquire the skills and technical knowledge to make these conjugations routine. We then functionalized the surface of Au nanoparticles with a protein called Apo-E, which is known to cross the blood-brain barrier (BBB) in rats. Working closely with researchers in the laboratory of Dr. Gunter Oberdorster we injected the functionalized nanoparticles into rats and harvested brain tissue for analysis. What we found was unexpectedly the Au nanoparticles functionalized with Apo-E did make it across the BBB, although the Au nanoparticles themselves are very large and should not cross the BBB. Further experiments are planned to understand the cause of the effect.

Novel Nanoparticle Synthesis

Nanoparticles (NPs) containing two completely different elemental compositions, (i.e. bi-functional nanomaterials), enable a single particle to have physical properties vastly superior to those made solely from the individual elements. We synthesized Au-Fe_2O_3 bi-functional nanoparticles by using a larger (50 nm) Au nanoparticle as a core surrounded by smaller (10 nm) Fe_2O_3 nanoparticles. We demonstrated the utility of these as-prepared Au-Fe_2O_3 nanoparticles by showing they can be used to separate proteins in solution. For example, bovine serum was efficiently removed from an aqueous solution with the simple addition of the NPs and application of a small magnet.

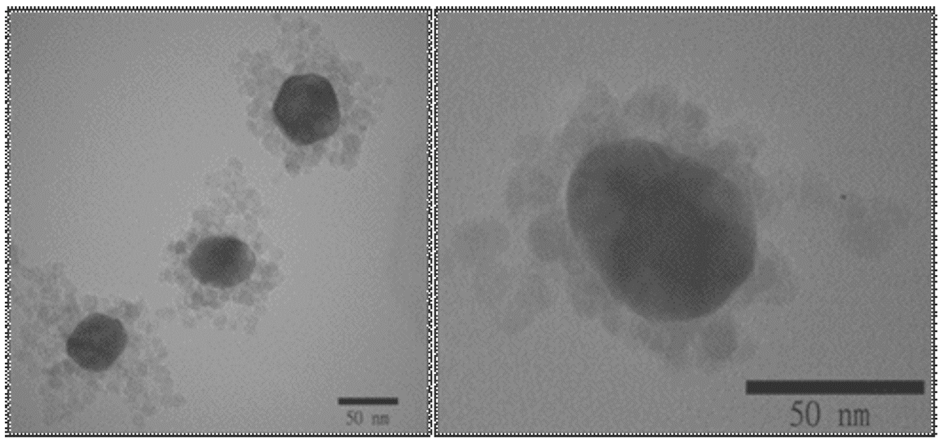

Figure 1. TEM images of a central 50 nm diameter Au nanoparticle surrounded by smaller ~ 10 nm diameter Fe_2O_3 nanoparticles forming a hybrid nanostructure.

We also discovered a facile, room temperature synthesis under ambient conditions of extremely small (diameter < 2 nm) PbSe quantum dot magic sized nanoclusters (MSCs) that emit in the near infrared with the remarkable property that their fluorescence fluorescence efficiency is typically >50% (Figure 2). These MSCs are unusually photostable for their size and can be easily transferred from organic to aqueous solutions while maintaining their high fluorescence efficiency (Figure 3). The aqueous MSCs also show excellent photostability (Fig. 2 inset), whereby under continuous photoexcitation the fluorescence intensity decreases only 40% over 6 hours.

An average hydrodynamic radius of 2.4 was measured for the aqueous PbSe MSCs by dynamic light scattering (Fig. 3). This work was performed on the Malvern Zetasizer that was purchased using funds from the MURI project. Such a small QD diameter is very significant, as these highly fluorescent MSCs are potentially small enough to be transported through the cell membrane or into the nucleus through carrier-mediated mechanisms, and future studies will address this possibility.

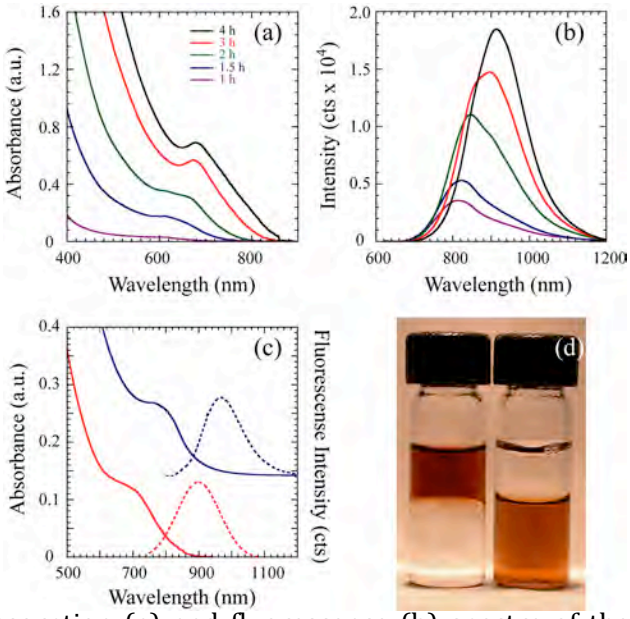

Figure 2. *In situ* absorption (a) and fluorescence (b) spectra of the PbSe QDNC growth solution over 4 h. (c) Absorption and fluorescence spectra of isolated QDNCs in tetrachloroethylene (TCE) (red) and water (blue). The absorption and fluorescence spectra red shift for QDNCs in water as expected.[15] (d) Picture of hydrophobic (left) and aqueous (right) PbSe QDNCs demonstrating excellent overall optical clarity.

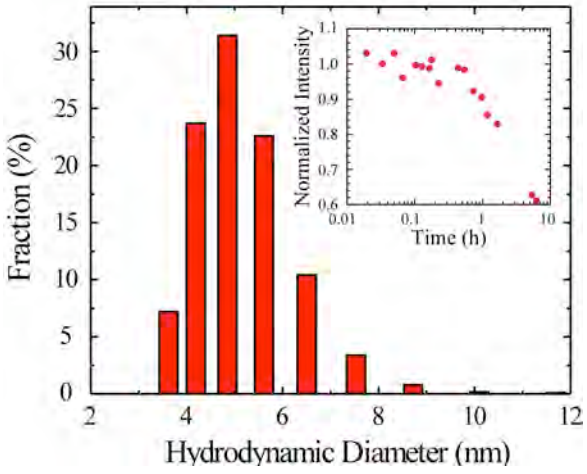

Figure 3. Hydrodynamic diameter for PbSe QD QDNCs exhibiting a distribution centered at 4.8 nm. The inset shows the fluorescence intensity of an aqueous solution of PbSe QDNCs under continuous laser excitation.

Carbon Nanotubes

We were also interested in the toxological effects of individual, isolated nanotubes on the cellular level. To conduct such studies requires the isolation of nanotubes in biologically compatible media, such as sterile saline. Nanotube isolation methods involve a vigorous sonication and centrifugation in the presence of surfactants, which being like soap tend to kill cells. Thus, we spent considerable effort looking for biological compatible surfactants that were simultaneously able to isolate individual nanotubes effectively in sterile saline solution. In summary, we found

that Tween-80 was able to solubilize relatively large amounts of isolated nanotubes in saline. We determined that nanotubes were indeed isolated by looking at absorption and fluorescence spectra from the single-walled nanotubes (Figure 4). As an added advantage, nanotube fluorescence is in the near infrared (~ 950 nm) in the biological transparency window, allowing for facile imaging.

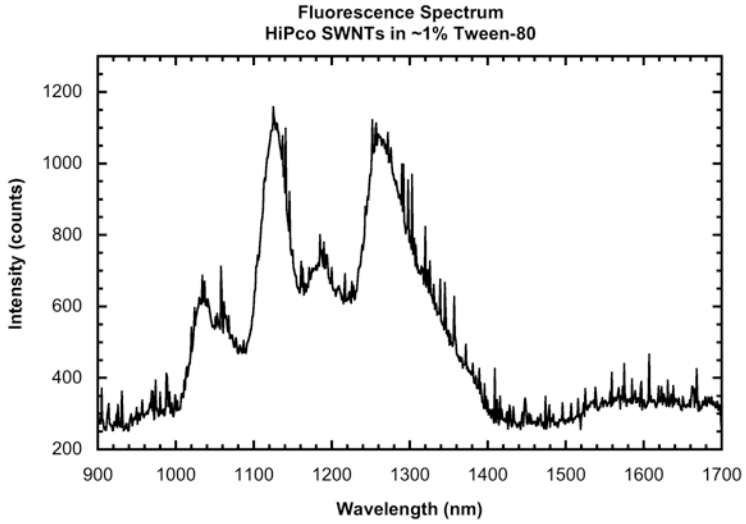

Figure 4: Fluorescence from individual single-walled nanotubes (SWNTs). The individual peaks in the spectrum correspond to different nanotube diameters and twists.

Honors:

Camille Dreyfus Teacher-Scholar Award (Krauss - 2005)
University of Rochester Goergen Award for Distinguished Achievement and Artistry in Undergraduate Teaching (Krauss - 2009)

Patents Filed

T. D. Krauss, L. Guo, J. J. Peterson, and C. Evans, "Quantum Dot Magic Size Nanoclusters, Uses, and Methods of Preparation Thereof," patent submitted (2008).

UNIVERSITY OF MINNESOTA
David Pui (dyhpui@tc.umn.edu)
Chen, Da-Ren

Postdoctoral Fellows:
Kim, Seong Chan
Qi, Chaolong

We have developed two systems to disperse nanoparticles and carbon nanotubes CNTs for realistic exposure studies. An in-vitro electrospray system was developed to delivered airborne nanoparticles to a tissue culture supported on a membrane. The membrane is placed on a Petri dish and is in contact with a culture medium of saline solution. This arrangement is essential to prevent cells from being desiccated. We have successfully deposited various nanoparticles, e.g., PSL, gold, Mn, MWCNT, on the targeted surfaces. An in-vivo electrospray system was developed to disperse airborne CNTs and TiO_2, QDs with various degrees of agglomeration for realistic exposure by animals. A mass throughput of 2 mg/m^3 of MWCNTs was achieved by this method. The system was used at the University of Rochester (Prof. Günter Oberdörster) for animal exposure experiments; the results were published in a journal paper in Nanotoxicology. A duplicate system was also used at the Institute of Inhalation Biology, Helmholtz Zentrum München (Prof. Wolfgang Kreyling). More details of the two systems are described below:

(1) *In vitro electrospray aerosolization*

The in vitro test system disperses nanoparticles by electrospraying a colloidal suspension, with deposition onto test samples. Figure 1a shows the electrospray system configured for the in vitro studies. A syringe pump feeds the nanoparticle suspension at a stable flowrate of 60 µl/hr through a metal capillary (125 µm I.D., 510 µm O.D.). A high voltage is applied to the metal capillary and can be changed from 3 to 5 kV depending on the electrospray jet shape, which can be visually monitored by a CCD camera. Due to the applied electric field, droplets generated by the electrospray are highly charged. The charges remain on the particles after the evaporation of the carrier liquid and maintain dispersion in the carrier gas. Industrial grade CO_2 is used as a carrier gas (1.0 l/min) to prevent the potential electric arcing at the metal capillary tip and to evaporate the carrier liquid in droplets prior to their arrival at the electrically grounded plate or the membrane film on the tissue culture insert.

The electrospray operating in the cone-jet mode occurs by the balance of divergent electric field and the surface tension of the droplet at the tip of the capillary, resulting in a liquid cone with a tiny jet emitted from the tip. The liquid jet breaks up into droplets with a narrow size distribution, with peaks ranging from 20 to 500 nm in diameter depending on the liquid conductivity and suspension flowrate. The monodispersity and high electrical charges of the electrosprayed nanoparticles enable them to be isolated, de-agglomerated during droplet evaporation, aerosolized, and then deposited on the test sample by the electrostatic force. Figure 1b shows the electrospray plume of Au nanoparticles when operated at the cone-jet mode.

For in vitro testing, it is essential to prevent cells from becoming dried out. Therefore, we designed a membrane deposition plate on a tissue culture insert to allow the cells to draw culture medium from their basolateral surfaces. Figure 1c shows the membrane on the tissue culture insert (TCI, Nalge Nunc, International) as the grounded plate where the test sample is placed and the nanoparticles are deposited. The membrane on the TCI, placed in a Petri dish, is in contact with a culture medium (saline solution). Electrical grounding of the membrane insert is done through the culture medium.

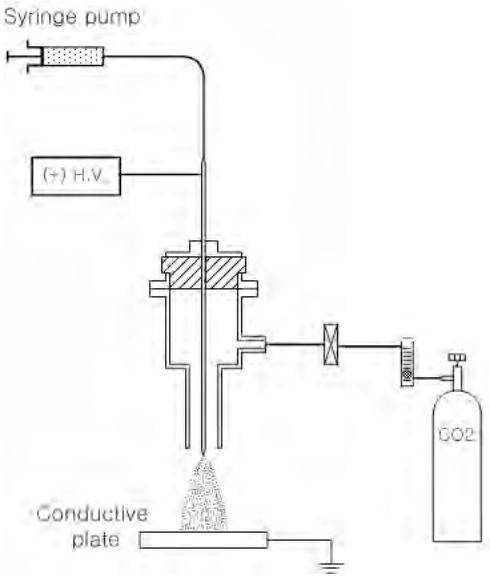

(a) *In vitro* electrospray system

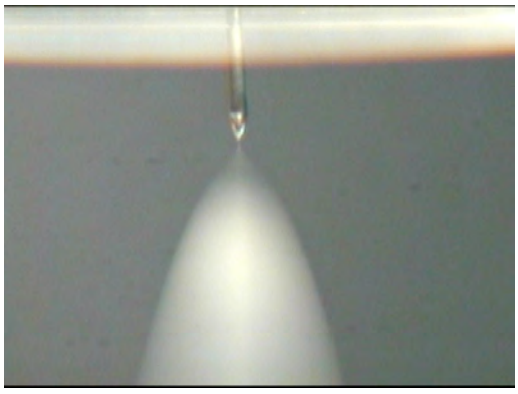

(b) Electrospray plume

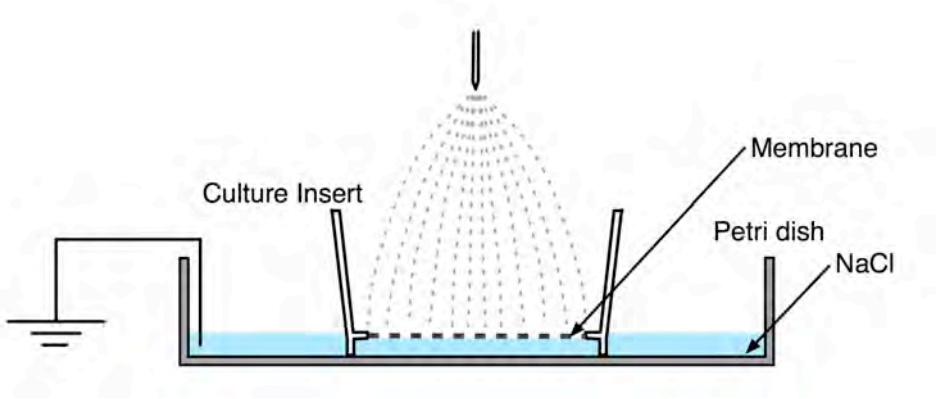

(c) Membrane deposition plate for *in vitro* test

Figure 1. *In vitro* electrospray system

The test nanoparticles included 50 nm PSL (Polystyrene Latex, 3050A, mean diameter: 46±2.0 nm, density: 1.05 g/cc, Duke Scientific Co.) (Figure 2a), 60 nm manganese (Mn_2O_3; Nanostructured and Amorphous Materials, Inc., Los Alamos, NM) (Figure 2b), 10 nm Au (GC 10, BBI International, Cardiff, United Kingdom) (Figure 2c). The test particles were suspended in 200 proof ethanol to decrease the liquid conductivity, thus enabling the electrosprayer to produce fine and uniform droplets. SEM and TEM images shown in Figure 2 demonstrate very uniform deposition of nanoparticles on the deposition plates. 10 nm Au nanoparticle suspensions were electrosprayed at the capillary tip with 20 mm height from the grounded plate, producing a deposition spot of 20 mm in diameter. The deposition rate of 10 nm Au nanoparticles was 29 ng/min (9 ng/cm^2 min). This can be varied by changing the liquid suspension flowrate, the spray tip height, the electrical conductivity of the sprayed suspension, and the applied voltage. A particle deposition model estimates that a human breathing 20 nm particles for 24 hrs with light exercise will deposit ~ 8 ng/cm^2 of alveolar surface; at rest, the model predicts the deposition to be ~3 ng/cm^2. Thus, the system is well-suited to investigating dose-related responses to nanoparticles in lung target cells.

The same system was also used for dispersing COOH functionalized MWCNTs (MS1233, purity: >95%, O.D.: 10~20 nm, I.D.: 5~10 nm, length: 10~20 μm, Timesnanoweb, China). Since the MWCNTs were supplied in a powder form, we established a procedure to disperse them in 200 proof ethanol (16 μg/ml) using a probe-type ultrasonicator (VCX-750, Sonic & Materials Inc., United State) with 750 watt for 1 minute to break up the MWCNT clumps before electrospray. The SEM image of the electrosprayed MWCNTs is shown in Figure 2d. The image shows a uniform deposition of individual CNTs over the entire deposition spot. The deposition rate was 16 ng/min (5 ng/cm^2 min); the total deposited mass can be increased by increasing the spray time.

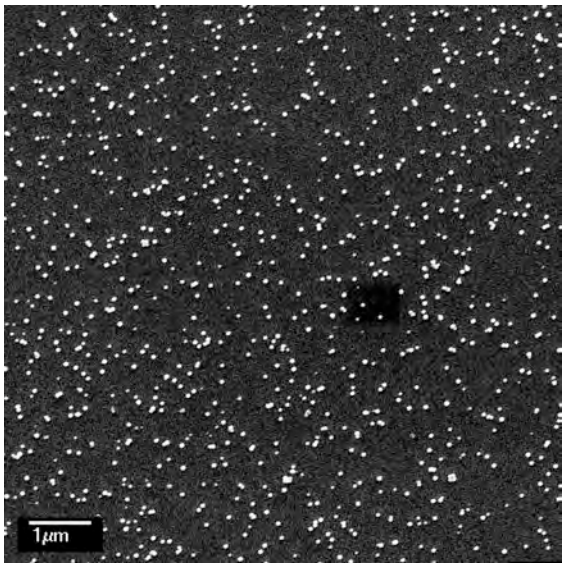

(a) 50 nm PSL NP

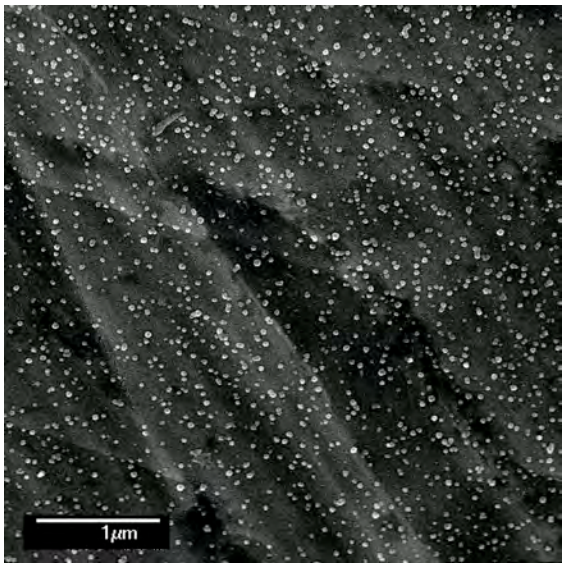

(b) Mn NP

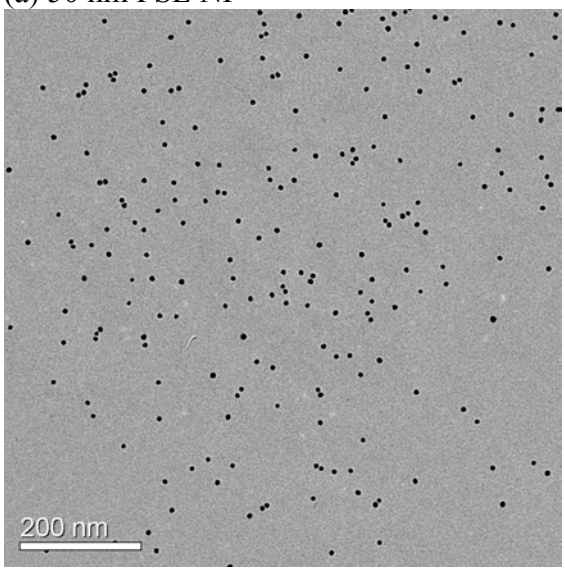

(c) 10 nm Gold NP

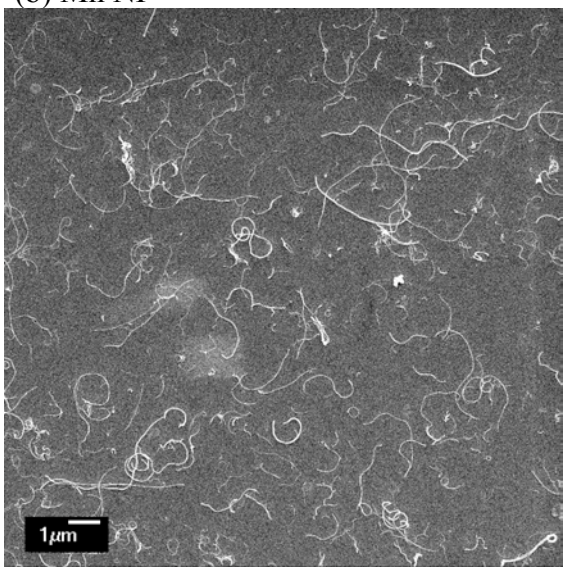

(d) Multi-wall CNT

Figure 2. EM images of electrosprayed nanoparticles (*in vitro* system)

(2) *In vivo electrospray aerosolization*

Figure 3 shows the electrospray system configured for in vivo exposures. A syringe pump is used to inject the nanoparticle suspensions into a metal capillary tube (I.D. 125 μm, O.D. 510 μm). High voltage is applied on the metal capillary to set up an electrical field between the capillary and a grounded orifice plate, and electrosprayed NPs pass through the orifice following the carrier gas. Due to the imposed electrical field during the spray operation, all the produced particles by electrospray are highly charged with the same polarity as that of the voltage applied on the capillary. Two Po-210 radiation sources with the activity intensity of 18.5 MBq per each were installed in a chamber next to the orifice plate to reduce electrical charges on gas-borne particles (thus to reduce the particle loss in the spray chamber). The sources emit α particles of high energy, ionizing air molecules and producing bi-polar ions. The operational condition of

the electrospray can be observed and monitored through the spray chamber window by a magnifying lens. The balance of the high electrical field with the liquid surface tension forms a cone shape of the liquid meniscus and the spray occurs near the cone tip, allowing controlled dispersion of nanoparticles in air.

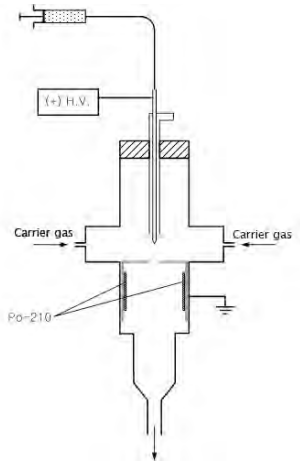

Figure 3. *In vivo* electrospray system

Au NPs, QDs, CNTs and titanium dioxide (TiO_2) nanoparticles were used with the system. Figure 4 shows airborne particle size distributions of the nanoparticles, as measured by an SMPS. A quantum dot sample (Q21531MP, 15 nm, PEG-amine, emission wave length: 565 nm, Invitrogen Co.) was electrosprayed after diluting one part sample with three parts ethanol. The peak in the SMPS measured size distribution (Figure 4a) is 13.6 nm. Electrosprayed CNTs have peaks at 41.1 nm for COOH functionalized single-wall carbon nanotubes (SWCNT, SS1214, purity: >90%, O.D.: 1~2 nm, length: 5~20 μm, Timesnanoweb, China) and 61.5 nm for COOH functionalized MWCNT, along with an impurity peak around 10 nm.

Suspensions of 60 nm and 80 nm Au nanoparticles (GC 60 and GC 80, BBI International, Cardiff, United Kingdom) were mixed with same volume of 200 proof ethanol prior to electrospraying; the peaks of the measured size distributions are 58.3 and 83.5 nm (Figure 4b) with particle mass concentrations of 1.5 and 2.5 $\mu g/m^3$, respectively.

The reasons for this low mass output include (1) the low Au NP concentration (GC 60 & GC 80: 57 μg/ml) in the original suspension, (2) low suspension feeding rate (60 μl/hr) of the in vivo electrosprayer, and (3) high particle loss by electrostatic force. With the modified in vivo electrosprayer (Figure 5), we can achieve a higher mass throughput up to 170 $\mu g/m^3$ by increasing the feeding rate (1 ml/hr) and removing the grounded orifice plate. In addition, we can achieve higher concentrations of airborne gold to several mg/m^3 by further concentrating the commercially available suspension of nanogold through centrifugation before suspending in alcohol for electrospray.

TiO_2 nanoparticles (P25, primary particle size: approximately 25 nm, Evonik Degussa, Germany) in powder form were dispersed in ethanol after ultrasonication. The peak of the size distribution (Figure 4c) appears around 60 nm, which is larger than the nominal primary particle size indicated in the product data sheet. The TEM image shown in Figure 4c suggests that the TiO_2 nanoparticles have a certain degree of aggregation in the original powder form due to the fusing of primary particles during formation. The

particle mass concentration for the TiO_2 can be increased up to 20 mg/m^3. Unlike with the other nanoparticle samples, we can generate high airborne concentrations of TiO_2 NPs even with an initial in vivo electrosprayer (Figure 3) because we can prepare highly concentrated suspensions (up to 20 mg/ml) that can be fed into the electrospray system.

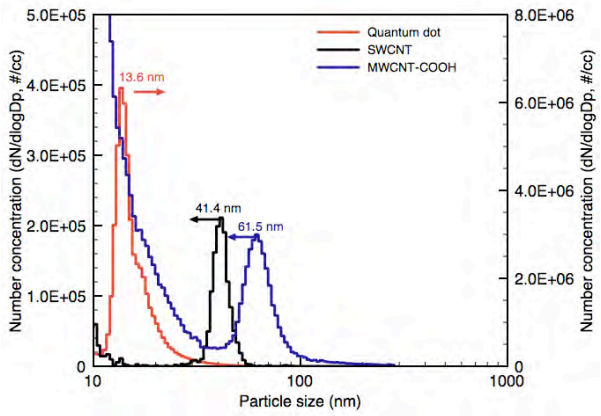

(a) Quantum dots and CNTs

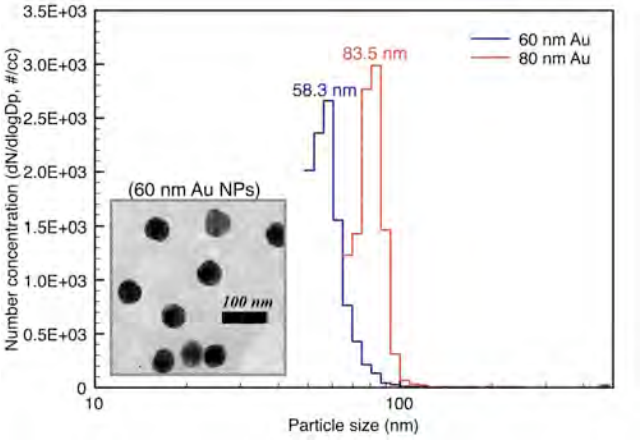

(b) Gold suspension

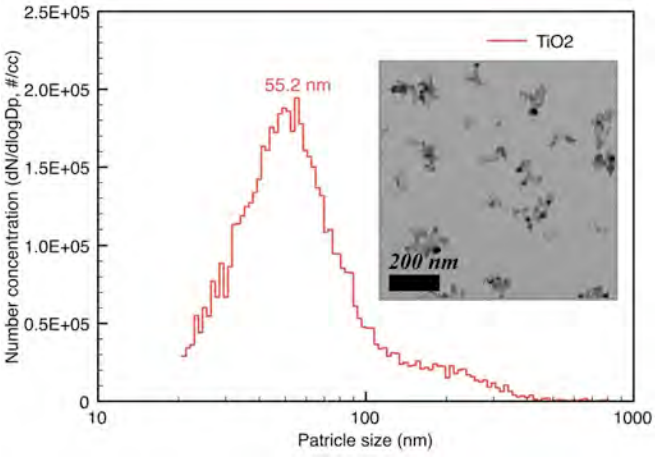

(c) TiO_2 suspension

Figure 4. Size distribution of electrosprayed nanoparticles (*in vivo* system)

(3) *Animal inhalation exposure test*

Figure 5 shows the animal inhalation exposure test system using an electrospray with a large capillary tube (I.D. 2.0 mm, O.D. 3.2 mm) to achieve higher throughput by increasing suspension flow rate up to 9 ml/hr and removing the grounded orifice plate which causes electrostatic particle loss around the edge and the lower side of the orifice. The electrospray capillary has a focusing shield (I.D. 6.35 mm) that provides a sheath air flow that keeps the spray angle narrow in order to reduce electrostatic particle losses in a grounded neutralization chamber and to minimize spray interference due to the high flow rate of the carrier gas. Four Po-210 sources (185 MBq each) are installed in the neutralization chamber in order to minimize electrostatic particle losses during the particle transportation to the animal inhalation chamber. The locations of radioactive sources in the neutralization chamber were carefully chosen to ensure that the entire charge-reduction zone is covered by α particles emitted from the sources while not allowing ions of opposite polarity of the applied voltage to travel upward to reach the spray capillary. This minimizes the potential interference of the spray process due to the neutralization of liquid meniscus surface.

The dispersion of several types of nanoparticles was tested with the system. For the animal inhalation exposure test, we selected multiwalled carbon nanotubes (MWCNT-7, O.D.: 50-85 nm, length: up to ~40 μm, Mitsui Co., Tokyo, Japan) that were first dispersed in 200 proof ethanol at a concentration of 0.1 mg/ml using a bath type ultrasonicator (Branson 1510) for longer than 24 hrs. The MWCNT mass and number concentrations were determined by measuring MWCNT deposition on a sampling filter and using a particle counter (CPC 3022, TSI Inc., Minneapolis, MN), respectively. In addition, particle size distribution was characterized using a Scanning Mobility Particle Sizer (SMPS 3936, TSI Inc., Minneapolis, MN).

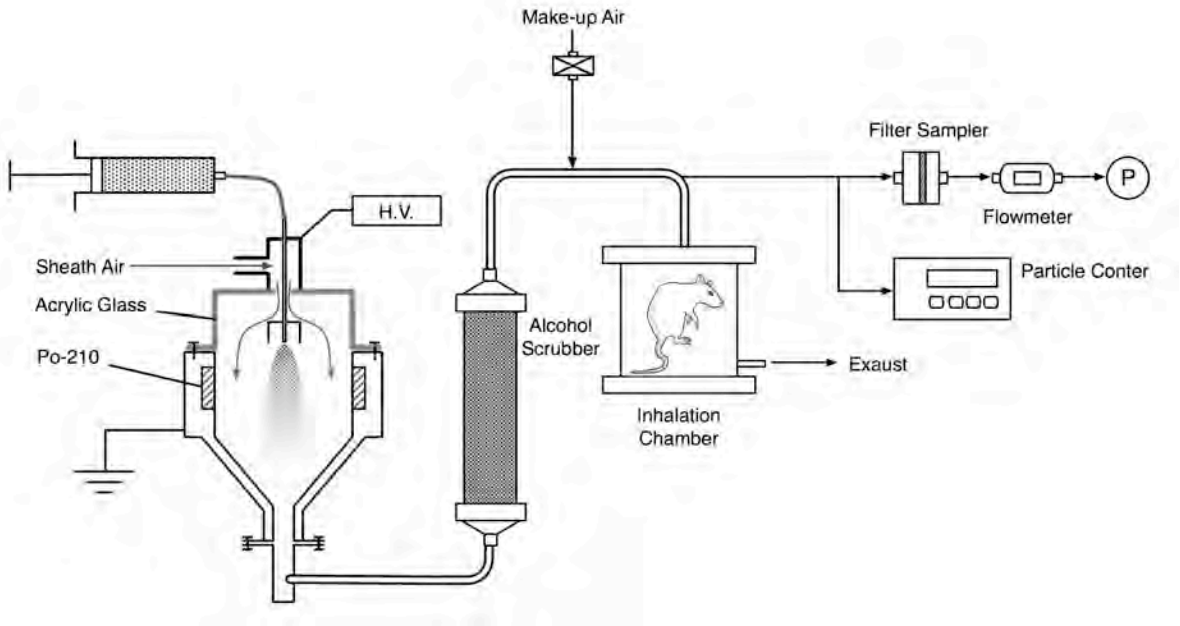

Figure 5. Animal inhalation exposure test system

We used ethanol as the carrier liquid to control the conductivity of the nanoparticle suspensions for electrospray operation and increase the dispersibity of MWCNT. However, the ethanol vapor in the aerosol will induce effects on the test animals and needs to be removed. Since the diffusion coefficient of ethanol vapor (1.47×10^{-5} m^2/s) is 200 times higher than that of 10 nm particles (5.4×10^{-8} m^2/s), the vapor can be efficiently removed by an activated carbon scrubber, as shown in Figure 4. The scrubber has four parallel meshed tubes embedded in activated carbon pallets. Ethanol vapor is removed by diffusion and absorption to the activated carbon pallets. The ethanol vapor removal efficiency was characterized by measuring the ethanol concentration via gas chromatography. The area of the ethanol peak was reduced by 99.7% when the ethanol vapor concentration before and after the scrubber was compared. The particle loss was less than 2% in mass through the scrubber.

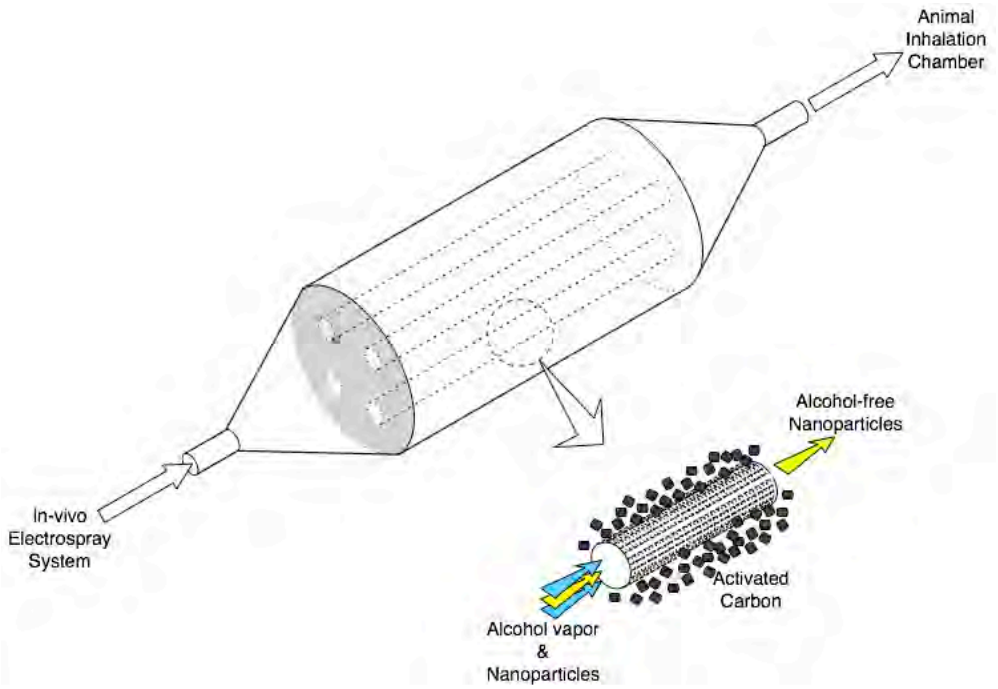

Figure 6. Activated carbon scrubber to remove unwanted chemical vapor

With the electrospray animal inhalation exposure system (Figure 5), we generated airborne MWCNT (MWCNT-7, Mitsui Co., Japan) with mass throughput of up to 2 mg/m^3, and a test rat inhaled the MWCNTs for 6 hours in the exposure chamber. Figure 7a shows the airborne MWCNT size distribution with a peak size of around 150 and 400 nm, which represent a single MWCNT peak and a MWCNT bundle peak. We can control the degree of agglomeration by changing the MWCNT suspension flowrate, because a higher flow rate generates bigger droplet sizes with more MWCNTs in each droplet. Figure 7b shows airborne MWCNTs sampled by an electrostatic precipitator with a suspension flow rate of 3 ml/hr, showing that the particles are well-dispersed and that some maintain a rigid, needle-like shape (asbestiform), which is a major concern of

MWCNT toxicity. Figure 7c shows the effect of a higher flow rate (9 ml/hr), which shows more agglomeration. By changing the degree of agglomeration of airborne MWCNTs, we can simulate more realistic conditions of CNT exposure studies.

In order to verify that electrosprayed nanomaterials were appropriately delivered to experimental animals, we used a suspension flow rate of 3 ml/hr to expose rats to the MWCNT for 4 hrs at a concentration of 800 $\mu g/m^3$. At 20 hrs post-exposure, animals were killed by an overdose of i.p. pentobarbital, the lungs were excised and lavaged 5 times with saline. After centrifugation (400 g, 10 mins) the lavaged cells were examined by light and scanning electron microscopy. Figures 7d and e show that alveolar macrophages contained the electrosprayed MWCNT, the shorter ones agglomerated inside macrophages and the longer ones were only partly phagocytized. Future studies with repeat exposures are planned to evaluate the lungs' responses to these realistically inhaled MWCNT as well as their translocation to extrapulmonary sites, specifically the visceral and parietal pleura as targets for induction of malignant tumors (mesothelioma) by biopersistent fibrous particles.

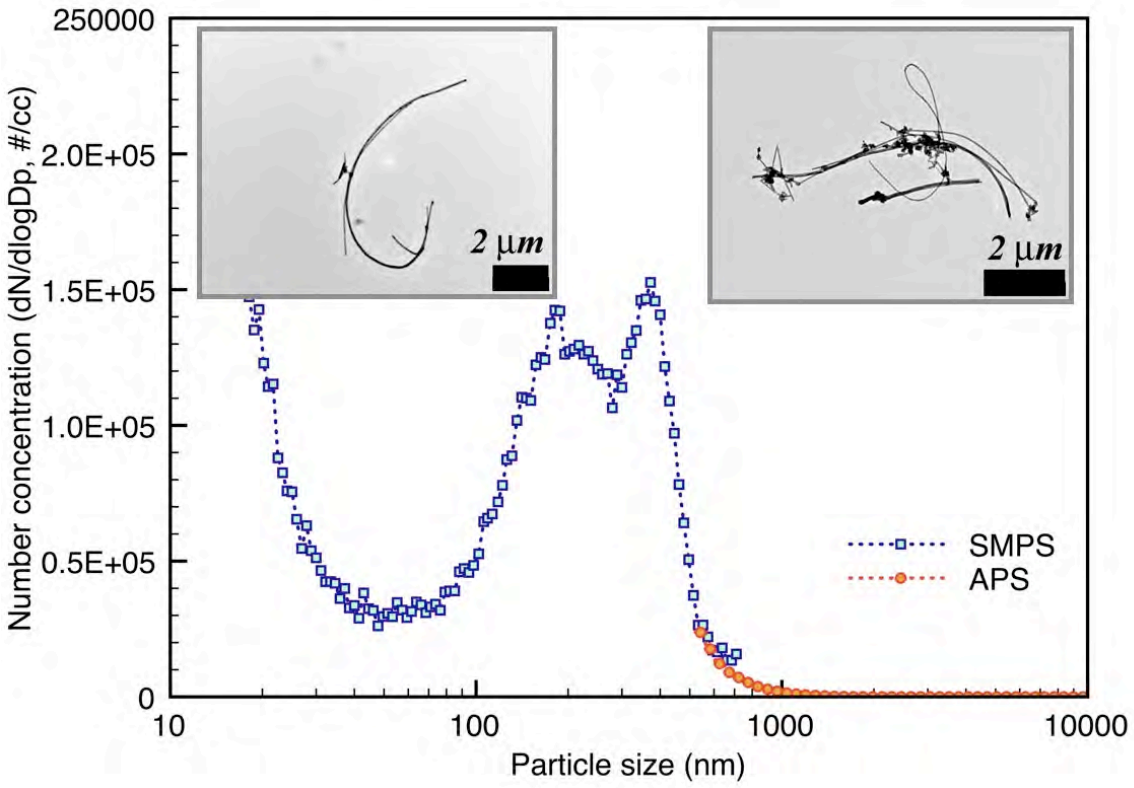

(a) Airborne MWCNT size distribution

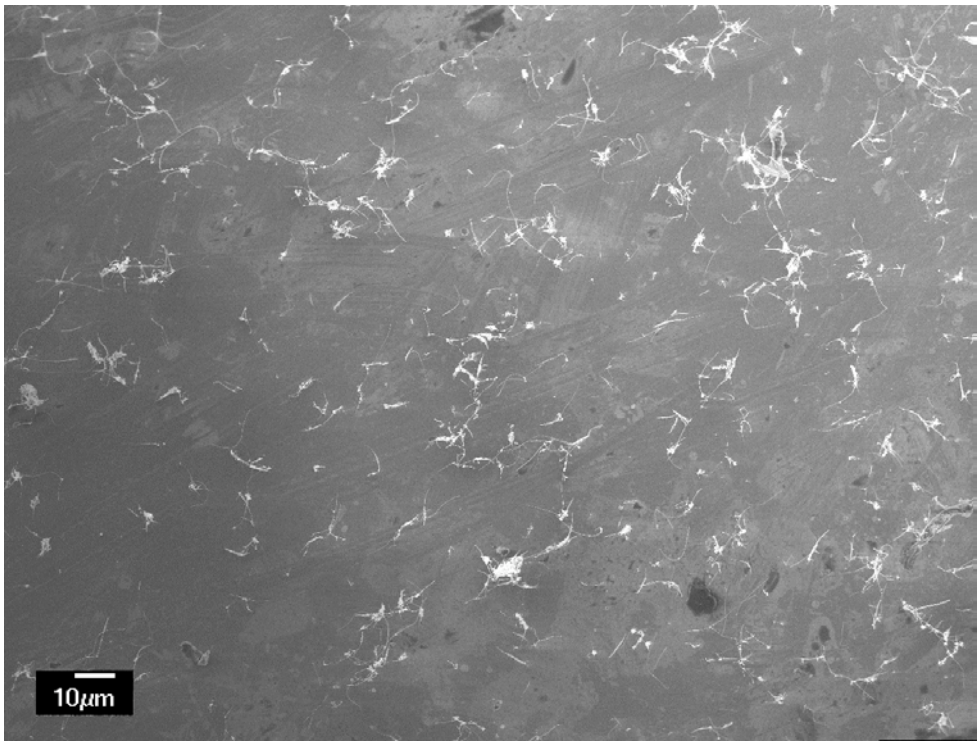

(b) Electrosprayed MWCNT for animal inhalation test (suspension flowrate: 3 ml/hr)

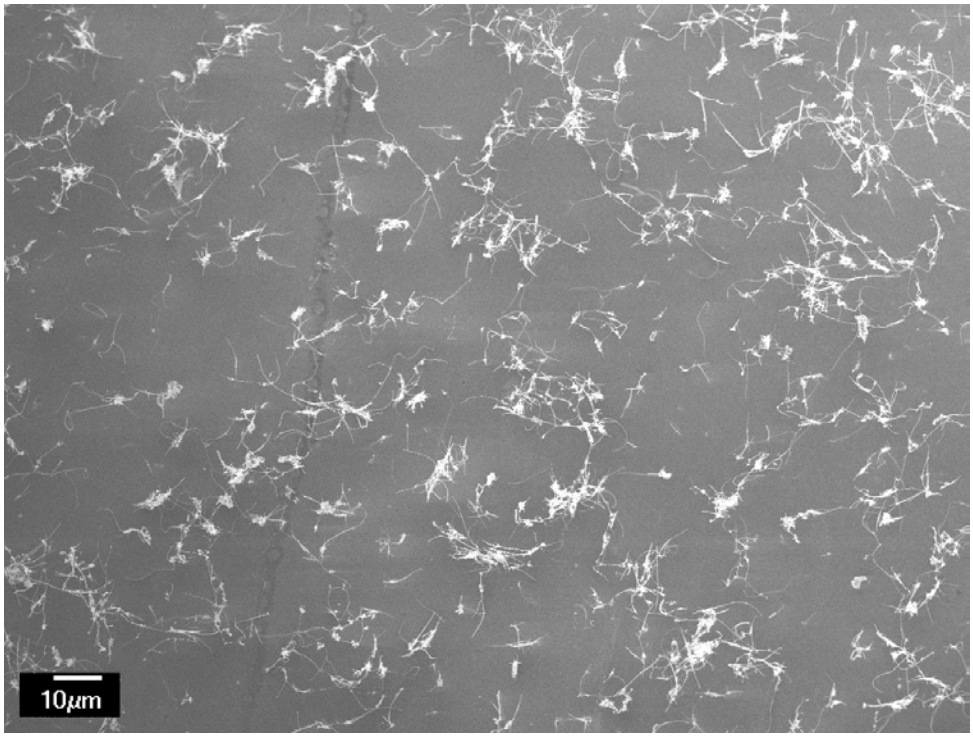

(c) Electrosprayed MWCNT for animal inhalation test (suspension flowrate: 9 ml/hr)

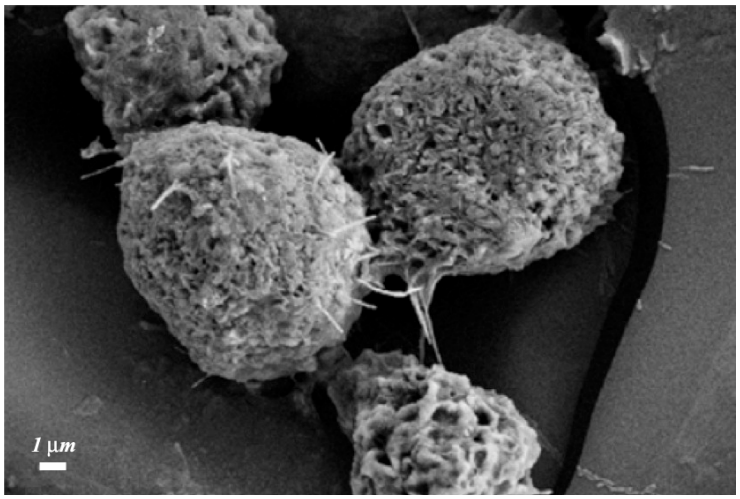

(d) Scanning electron microscopic of rat alveolar macrophages in lung lavage fluid 20 hrs after electrospray inhalation exposure to MWCNTs

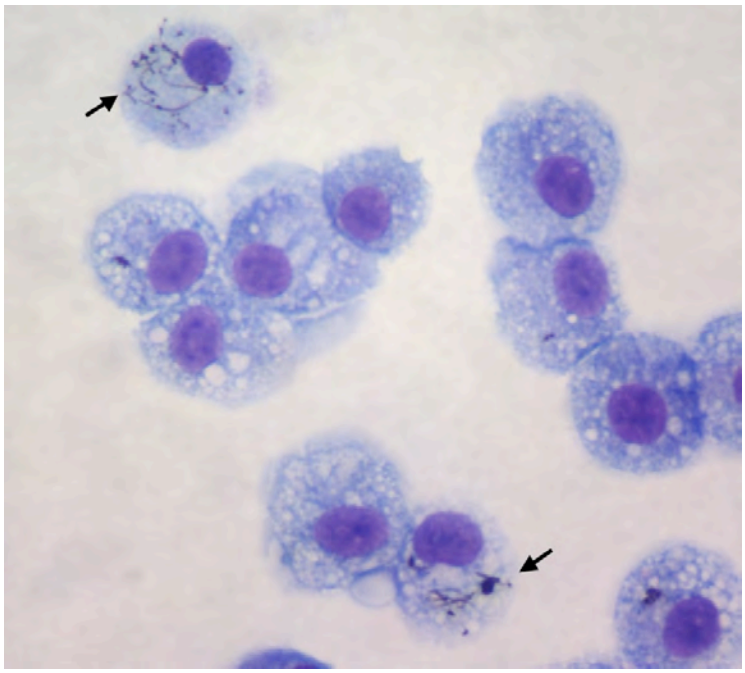

(e) Light microscopic image of rat alveolar macrophages in lung lavage fluid 20 hrs after electrospray inhalation exposure to MWCNTs

Figure 7. Animal inhalation test results

(4) *Alternative method for Ag/Au NP generation*

Commercially available Ag or Au suspensions are suspended in surfactants with low number concentration in order to prevent nanoparticles from being agglomerated during storage time. However, this results in low airborne NP concentration even with minimum particle loss in the electrospray system. So we needed to develop an alternative method replacing electrospray system. Figure 8a shows a dual electric furnace system for

Ag NP generation. The silver powder source located in the center of a heating tube is vaporized and condensed into spherical Ag nanoparticles. The primary particle size can be adjusted by changing the heating temperature, e.g. lower temperature generates smaller and less NPs and vice versa. Figure 8b shows 10 nm Ag NPs distribution with the heating of 1,000 °C, and the mass concentration is 156 μg/m3. In order to get larger spherical Ag NPs, we used an agglomeration and sintering process. The primary particles stick upon collision to form NP agglomerates in an agglomeration chamber located in the downstream of the primary particle generation furnace. The agglomerate size increases by increasing the primary particle number concentration and the residence time in the agglomeration chamber. In Figure 8c, the chamber volume is 1.7 liter and the residence time is approximately 2 min. Downstream of the chamber, the NP agglomerates are sintered in a second furnace for spherical NPs. Figure 8c shows 50 nm Ag NPs distribution generated by the first furnace of 1,100 °C and sintered by the second furnace of 600 °C, and the mass concentration of 50 nm Ag spherical particle is 7 mg/m^3.

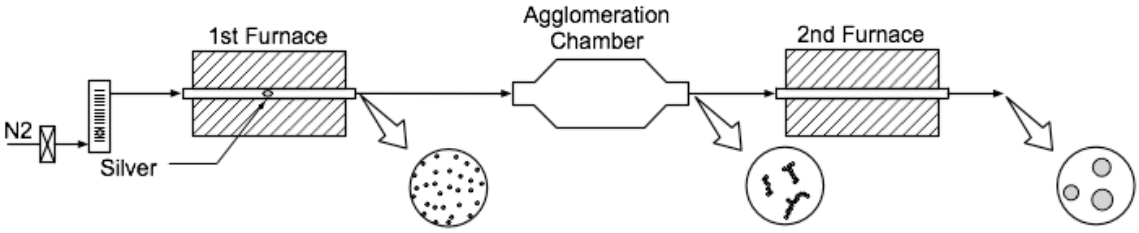

(a) Ag NP generation system using dual furnaces

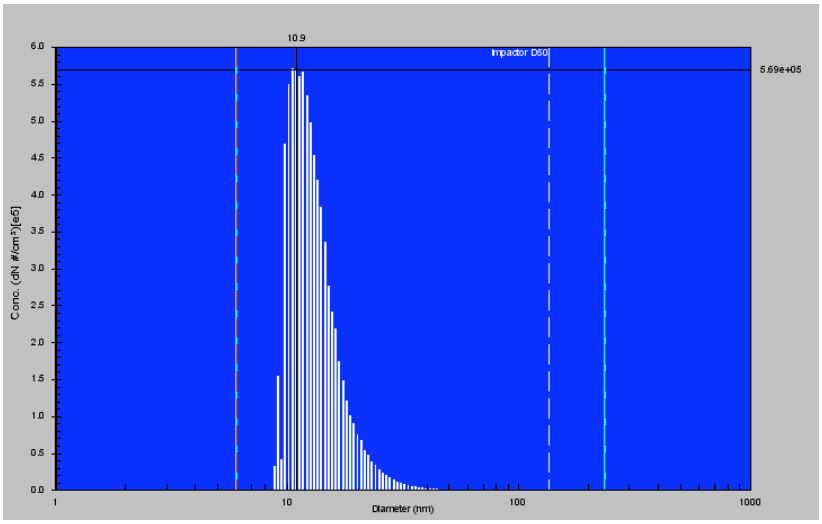

(b) 10 nm Ag NP generated by an electric furnace

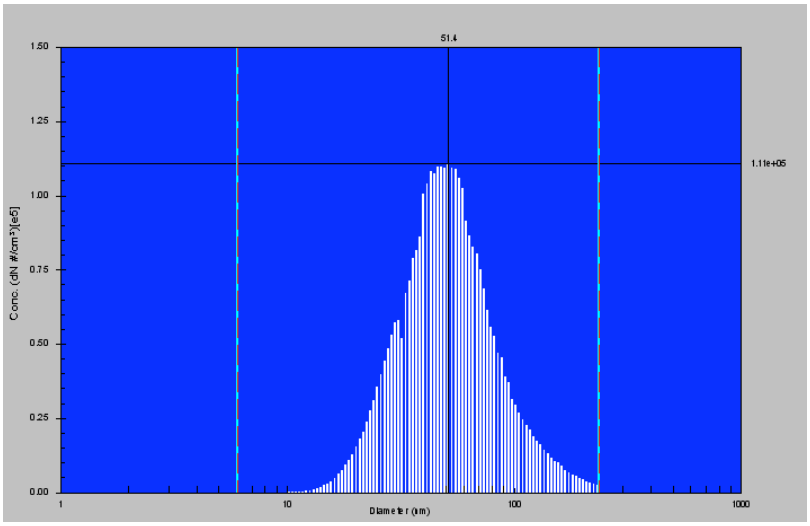

(c) 50 nm Ag NP generated by dual furnaces

Figure 8. Ag NP generation using dual furnace system

Au has higher melting point (1,064.18 °C) than Ag (961.78 °C), and needs higher temperature to generate NPs using an electric furnace, which means we need a high capacity furnace to generate large Au NPs. So we used a spark discharge method to generate Au primary particles and increase the NP size using an agglomeration chamber with a sintering furnace (Figure 9a). The spark discharger (GFG-1000, Palas) uses high voltage to generate high frequency sparks between two conductive rods with controllable frequency. The resulting vaporized Au condenses to very fine particles, which coagulate to form agglomerates during further transport. The particle mass flow rate is adjustable by varying the spark frequency. 10 nm of primary particles can be generated with 50 Hz of a spark frequency, and with higher spark frequency the mean particle size increases due to an agglomeration of the primary particles. In order to increase the particle size even higher, we use an agglomeration chamber (10 liter) after the spark discharger, then sinter the NP agglomerates into spherical particles using a sintering furnace. The final size of the spherical particle can be decided by a spark frequency and a residence time in the agglomeration chamber. Figure 9 b and c show NP size distribution change before and after the sintering furnace. With 1 kHz of spark frequency and 1 lpm of total flowrate (residence time: 10 min.), the mean size of agglomerate was measured around 115 nm, and after sintering at 600 °C the particle morphology changed into sphere with mean size of 43 nm.

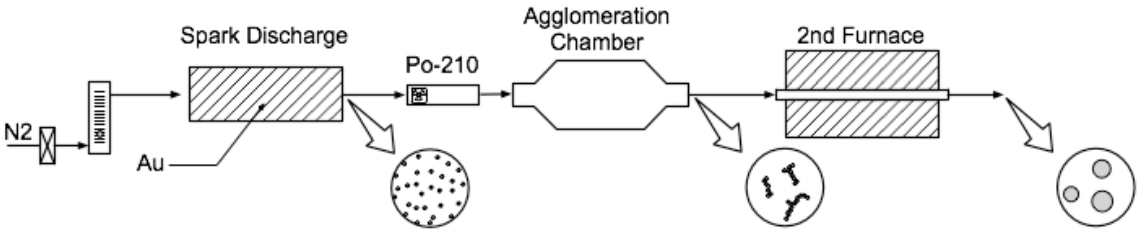

(a) Au NP generation system

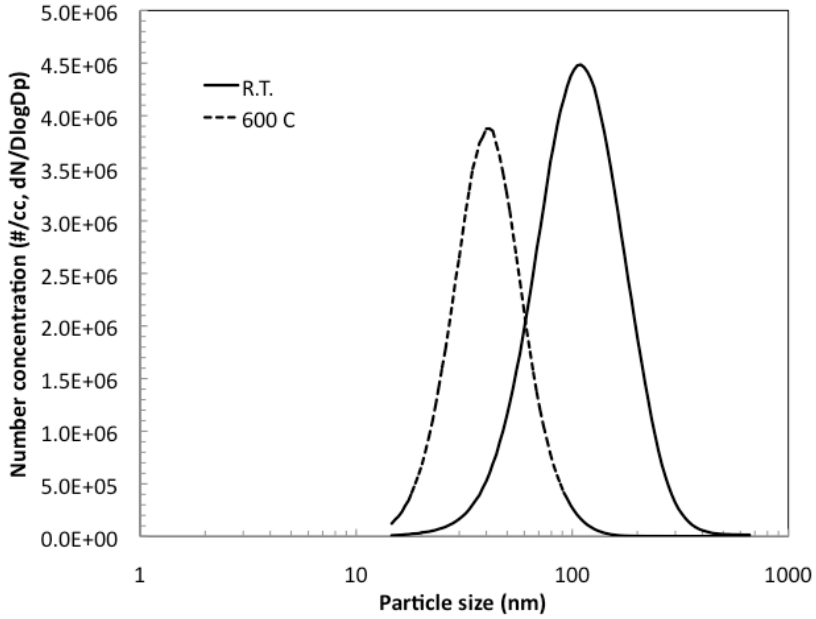

(b) Size distribution change by sintering

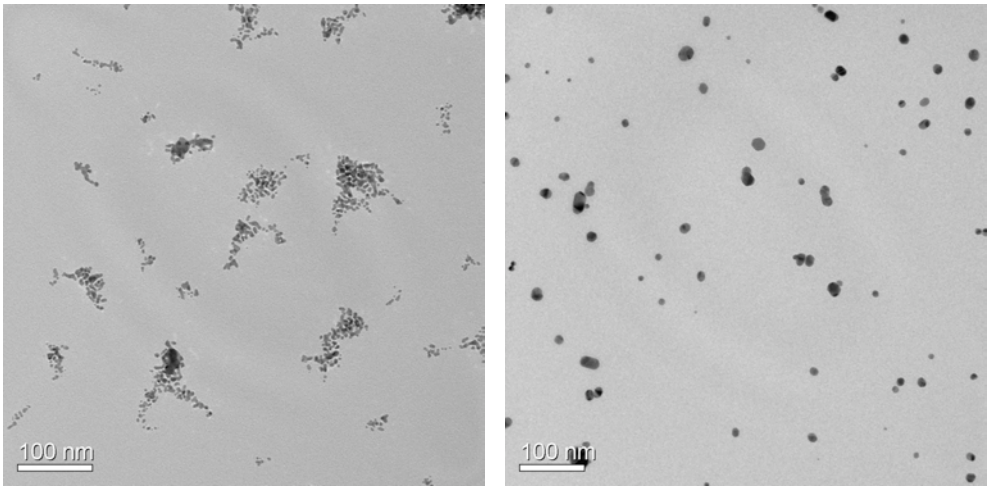

(c) Morphology change (left: room temperature, right: sintering at 600 °C)

Fig. 9. Au NP generation by spark discharge/sintering

WASHINGTON UNIVERSITY IN ST. LOUIS

Pratim Biswas (pratim.biswas@seas.wustl.edu)
Daren Chen

Postdoctoral Fellows:
Zhu Liying
Chen Xu

Students:
Jiang Jingkun
Sahu, Manoranjan
Fan Mei

OBJECTIVES/KEY FINDINGS/RESULTS/ACCOMPLISHMENTS

The work conducted and findings can be categorized in three areas: (i) characterization of synthesized nanomaterials (primarily from different commercial sources) prior to biological studies, and (ii) synthesis of well controlled nanomaterials in gas phase reactors for biological studies. (iii) electrospray based delivery systems for exposure studies

The key findings in (i) Nanomaterials including silver, gold, platinum, copper, carbon nanotube, cadmium selenide, aluminum oxide, manganese oxide, silicon dioxide and titanium dioxide are characterized by the established routine approach, which were used in the vitro and in vivo studies at U of Rochester. This approach includes x-ray diffraction to determine the crystal structure, BET analysis to determine the surface area and porosity; electron microscope analysis to determine the morphology (i.e. Figure 1 for commercial TiO_2 nanowires) and confirm the primary particle sizes; and scanning mobility particle size distribution analysis to obtain the size distribution on aerosolization of the nanomaterial. These analyses help to establish the relationship between physicochemical characteristics and toxicological properties of nanomaterials. Another important finding is that often manufacturer specifications do not match the characteristics of the nanoparticles, or that these characteristics change with time. The third important finding is that that characteristics of nanomaterials that are commercially produce often do not match what is measured under careful conditions in our facilities, Thus, the importance of characterization prior to toxicological studies is paramount.

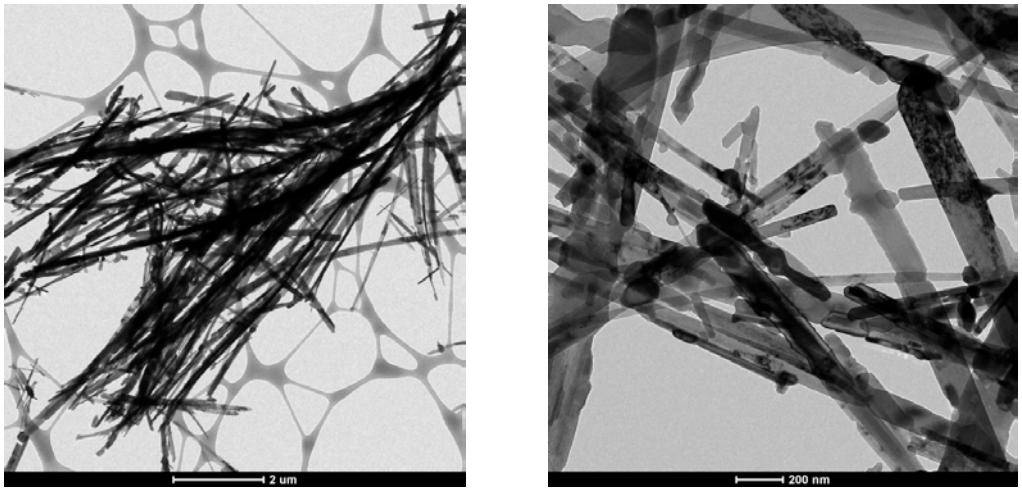

Figure 1. TEM images of TiO2 nanowires with different magnification

(ii) Synthesis of well controlled nanomaterials in gas phase reactors for biological studies.

(ii-1) TiO_2 nanoparticles synthesized by FLAR, characterization and the correlation study between physic-chemistry properties and toxicity.
Well controlled TiO_2 nanoparticles were synthesized in flame aerosol reactors (Figure 2) and in-house developed multi-stage differential mobility analyzer (MDMA) was used to produce monodisperse nanomaterials (Figure 3).

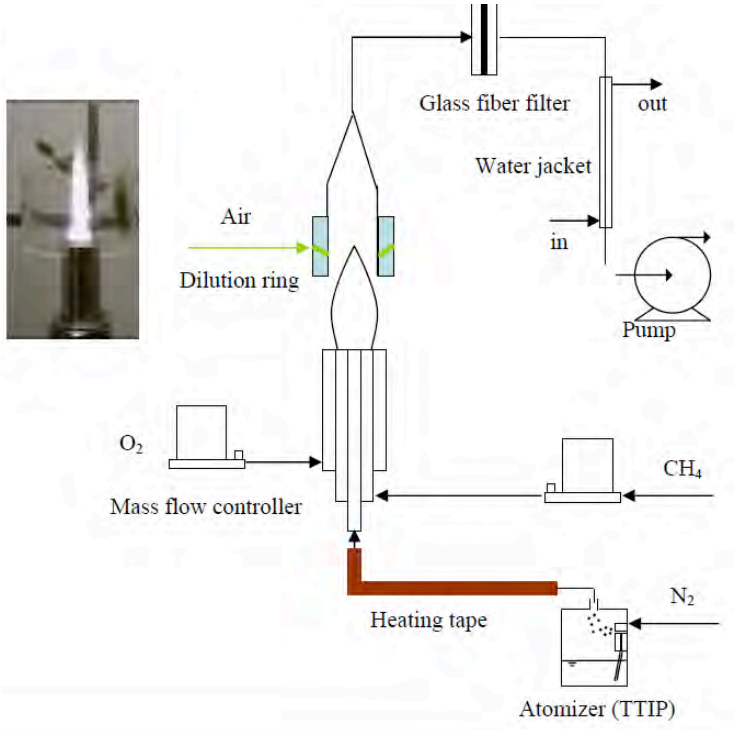

Figure 2. Schematic diagram of flame aerosol reactors (FLAR)

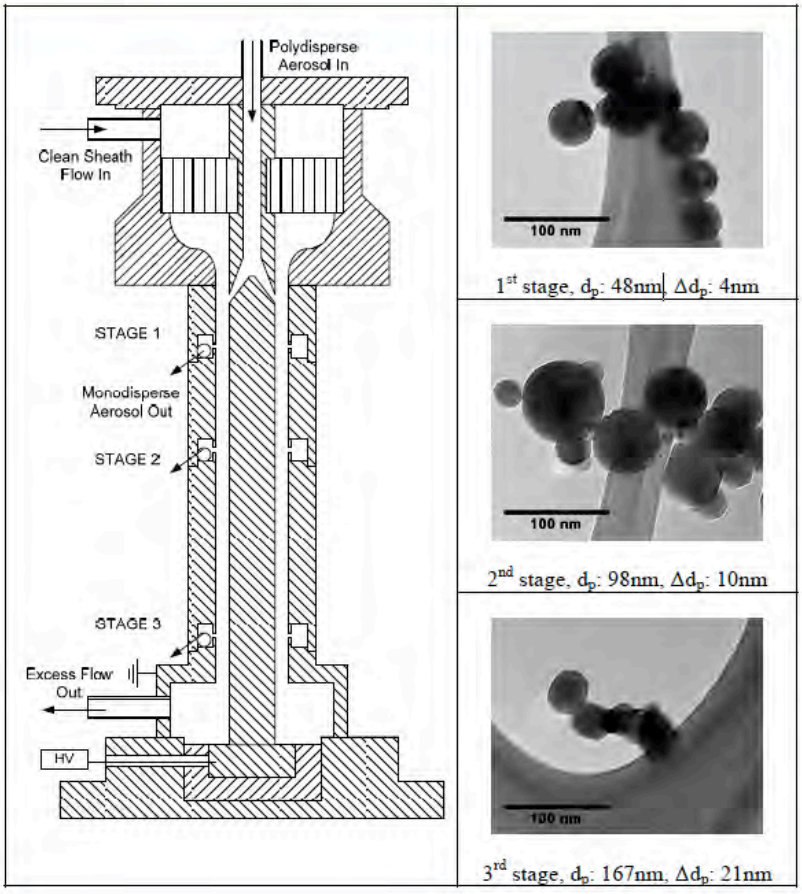

Figure 3. Monodisperse nanoparticles produced in MDMA (1st stage)

The understanding of the nanoparticle synthesis process has allowed us to design systems to produce high quality nanomaterials for biological studies. Two notable sets of samples are prepared. The first set was TiO_2 retaining the same crystallinity anatase but different size with a range of sizes from 3 nm to 200 nm. The second set was to vary the crystallinity for the same size nanoparticle and 8 samples with different ratios of anatase to rutile were produced. Such a large number of well characterized samples have not been used by any other research group in such toxicological studies. Dr. Oberdörster's group conducted the biological test and the correlation between toxicity and crystallinity/size of TiO_2 was established (Figure 4 and 5).

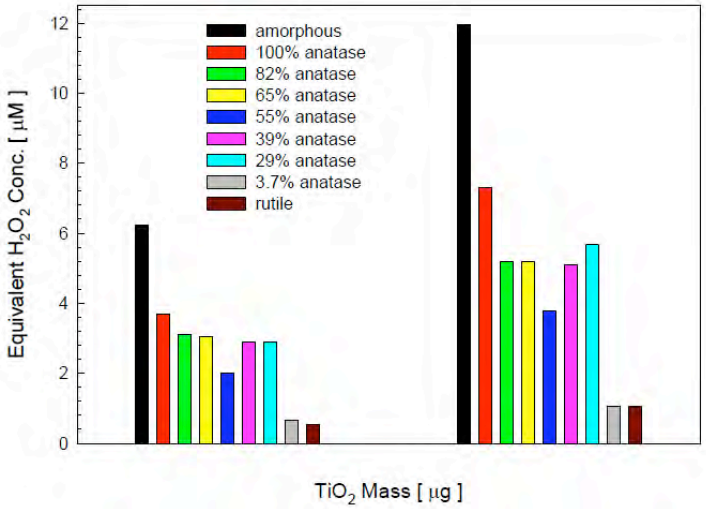

Figure 4. The activity of TiO_2 with different crystallinity

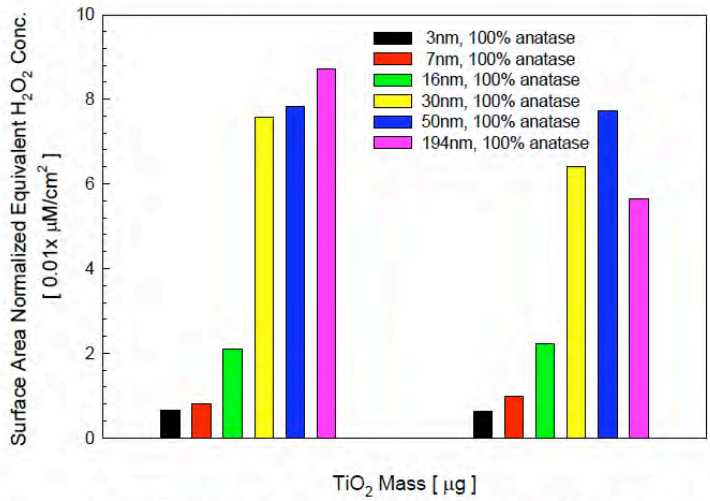

Figure 5. The activity of TiO_2 with different size but same crystallinity

In order to investigate a detailed evaluation of ROS activity as a function of physico-chemical properties, with the same synthesis method, 16 different TiO_2 samples were synthesized with tight control on characteristics. (Table 1) To establish the true effect of particle size, different metrics were examined – and it was established that the ROS generation per surface area allowed for a clear understanding of the trends. A S-shaped curve for ROS activity per area as a function of particle size was obtained for the same crystal phase of titanium dioxide nanoparticles. For particles larger than 30 nm, the activity per unit area was constant, followed by a decrease when particle size decreased from 30 nm to 10 nm, and constant values for particles smaller than 10 nm. It is expected that all nanoparticles would exhibit a similar behavior, however, the dependence is a strong function of the exact synthesis procedures used. Such S-shaped curves may also be used to more precisely define particle sizes of importance; for example, greater than 30 nm being defined as bulk sizes, between 30 and 10 nm as the nanometer size

regime, and less than 10 nm as the quantum regime (rather than an arbitrary definition for all nanoparticles to be less than 100 nm). The toxic potential exhibited by TiO_2 particles with similar size but different crystal structures was highest for amorphous samples, followed by pure anatase, and lower for anatase/rutile mixtures, and lowest for pure rutile.

Table 1. 16 different TiO_2 samples synthesized with tight control on characteristics.

No.	Crystal Phase	S_A[a] (m^2/g)	d_{BET}[b] (nm)	d_p[c] (nm)	d_{XRD}[d] (nm)	Synthesis Method
1	100% anatase	426.1	4	5 ± 1	3.2	e
2	100% anatase	209.6	7	8 ± 2	7.7	e
3	100% anatase	155.7	10	11 ± 3	10.4	e
4	100% anatase	95.80	16	15 ± 4	19.7	e
5	100% anatase	51.93	30	30 ± 9	29.1	f
6	100% anatase	38.86	40	40 ± 12	30.3	f
7	100% anatase	31.52	50	48 ± 14	41.2	f
8	100% anatase	14.99	104	98 ± 29	42.0	f
9	100% anatase	8.033	195	182 ± 29	67.1	g
10	82% anatase/ 18% rutile	25.48	60	56 ± 17	40.9	f
11	80% anatase/ 20% rutile	57.44	27	26 ± 8	23.1	h
12	65% anatase/ 35% rutile	29.27	51	53 ± 16	41.0	f
13	61% anatase/ 39% rutile	38.08	39	38 ± 11	31.8	f
14	55% anatase/ 45% rutile	35.95	41	40 ± 12	32.9	f
15	40% anatase/ 60% rutile	38.23	38	40 ± 12	31.3	f
16	39% anatase/ 69% rutile	31.37	47	45 ± 13	32.7	f
17	29% anatase/ 71% rutile	43.12	34	35 ± 10	26.9	f
18	4% anatase/ 96% rutile	19.43	73	-	32.1	i
19	100% rutile	13.78	102	-	-	i
20	amorphous	482.3	3	-	-	j
21	amorphous	34.33	41	45 ± 13	-	k
22	amorphous	26.67	53	59 ± 21	-	k

[a] Specific surface area of particles as measured by N_2 adsorption (BET). [b] Equivalent particle diameter as calculated from the specific surface area. [c] Primary particle size as determined by electron microcopy. [d] Particle crystallite size (anatase) as determined by X-ray diffraction (XRD). [e] Premixed flame aerosol reactor. [f] Diffusion flame aerosol reactor. [g] Commercial available (Fisher Scientific). [h] Commercial available (Degussa P25). i Annealed in the furnace reactor. j Spark aerosol generator. k Furnace aerosol reactor.

Though only chemical activity was measured, this is very relevant to toxicological studies. The intrinsic non-biological reactive oxygen species generation could be used as a pre-screening strategy to examine nanoparticle toxic potential. However, the validity of this suggestion needs to be determined in subsequent toxicity tests using a range of particle sizes (<10 nm to >30 nm) with well defined crystal structure in cell and animal studies. The method of presenting the data proposed in this paper allows to evaluate the true effects of parameters such as size. For example, to study the effect of size, the biological signal (such as inflammation, neutrophil generation or others) should be presented per unit surface area for the different sizes. This will allow to unravel the true effect of size, or any other parameter. If the trends do not follow that of the chemical activity measurements

(for example, the S-shaped curve (Figure 6) as determined by ROS measurements), then the results need further interpretation and could be caused by other effects. For example, agglomeration of particles could be one important factor. All the particles used in this study tended to agglomerate to different degrees in solution (the hydrodynamic sizes of 10 nm and 50 nm particles in deionized water are 140 nm and 525 nm, respectively). While not important in establishing chemical activity relationships as the surface of the particle is still available, it may be a very important factor to influence the results of the *in vivo* or *in vitro* studies.

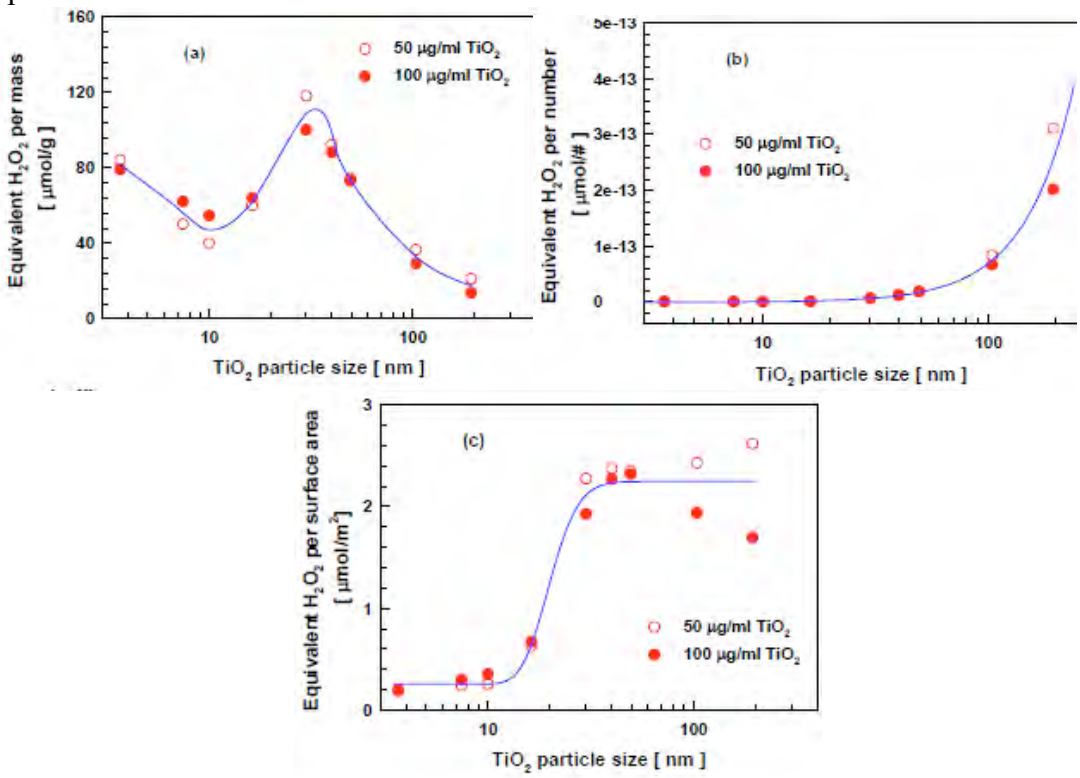

Figure 6. Reactive oxygen species (ROS) generated by anatase TiO_2 particles of different sizes (No. 1 - 9) normalized by several different dose metrics: (a) particle mass concentration; (b) particle number concentration; (c) particle surface area concentration

(ii-2) Doped Nanomaterials

While pristine nanoparticles are used for toxicity studies, in many applications, doped nanomaterials will also be used.A diffusion flame aerosol reactor was used to extend the synthesis from the pure TiO_2 to Cu-doped TiO_2 nanomaterials. These doped nanomaterials currently being used for increasing the performance in various applications. The synthesized materials were extensively characterized by using techniques such as X-ray diffraction (XRD) pattern for determining the crystal phase, transmission electronic microscopy (TEM) and scanning electronic microscopy (SEM) for the morphology, and UV-Vis spectrum for light absorption (band gap identification) and dynamic light scattering to understand the aggregation behavior. The properties of

the nanomaterials such as size, crystallinity, and morphology were well controlled by understanding the formation and growth of nanoparticles in the high temperature flame. The important process parameters controlled were: molar feed ratios of precursors, temperature, and residence time history in the high temperature flame. Results indicate that with increasing copper dopant concentrations caused anatase to rutile phase transformation and decreased crystalline nature and primary particle size. The increase in doping concentration caused the transformation from anatase to rutile phase of TiO_2 due to replacements of Ti^{4+} atoms by Cu^{2+} atoms in the crystal structure of TiO_2 and resulted in a decreased primary particle size. Absorption spectroscopy measurements confirm a shift in the absorption wavelength, caused due to crystal structure modification, by potentially replacing copper ions in the TiO_2 crystal structure.

Nanoparticles having different chemical composition, size, surface structure, shape and aggregation in the aqueous medium are expected to have different interaction mechanisms and biological effects. For toxicity evaluation Cu-doped TiO_2 nanoparticles properties were strictly controlled. To evaluate the role of chemical composition (i.e. dopant concentration) on Cu-doped TiO_2 nanoparticles toxicity composed of same crystal structure and similar primary particle diameter and to evaluate the particle size and crystal structure effects in Cu-doped TiO_2 toxicity at a fixed chemical composition. The copper dopant concentration was varied from 0 to 7 wt% with primary particle size of ~35nm and anatase crystalline structure. The XRD pattern of the doped nanoparticles are shown in Figure 7 and the representative TEM micrographs and size distribution of the doped nanoparticles are shown in Figure 8. The particle size with anatase crystalline structure was varied from 15nm to 70nm and the phase composition was varied from 39% to 100% anatase maintaining the particle size similar (~35nm) at 3 wt% dopant concentration.

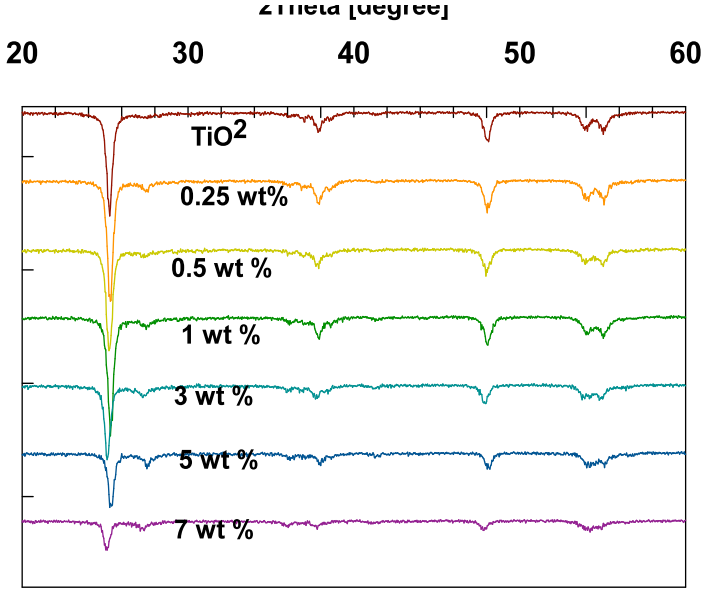

Figure 7. XRD spectra of as-prepared pristine TiO_2 and Cu-doped TiO_2 nanoparticles with different dopant composition

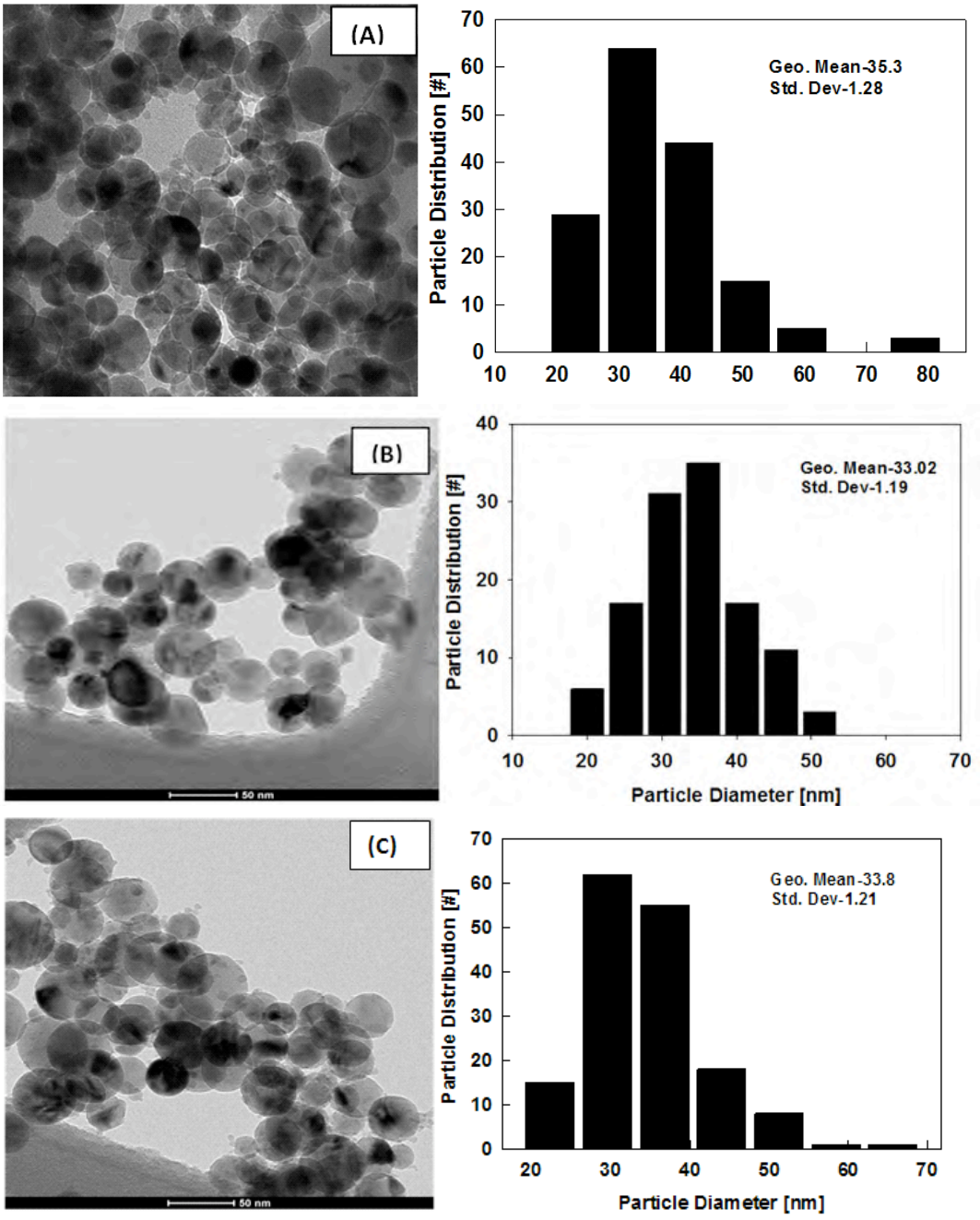

Figure 8. TEM and particle size distribution of representative pristine TiO_2 and Cu-doped TiO_2 nanoparticles with dopant composition (A) Pure TiO_2 (B)1 wt% Cu-TiO_2 (C) 3 wt% Cu-TiO_2

(iii-3) Properties of nanomaterials in suspension

Another key aspect of the study was to evaluate the role of nanoparticles in suspension. While using novel aerosol routes to generate these nanomaterials resulted in the ability of production of well tuned samples; the eventual fate in the aqueous suspension is of importance. Extensive studies were conducted using DLS (dynamic light scattering) systems to evaluate agglomeration behavior in suspension. Due to the hydrolysis reactions, a negative surface charge resulted on the surface of the nanoparticles. The resultant double layer thickness varied depending on the solution ionic strength. As a result, various hydrodynamic diameters were obtained. Agglomeration was found to be very prevalent in these systems.

Characterizing the state of nanoparticles (such as size, surface charge, and degree of agglomeration) in aqueous suspensions, and understanding the parameters that affect this state are imperative for toxicity investigations. The role of important factors such as solution ionic strength, pH and particle surface chemistry that control nanoparticle dispersion was examined. The size and zeta potential of four TiO_2 and three quantum dot samples dispersed in different solutions (including one physiological medium) were characterized. For 15 nm TiO_2 dispersions, the increase of ionic strength from 0.001 M to 0.1 M led to a 50 fold increase in the hydrodynamic diameter; and the variation of pH resulted in significant change of particle surface charge and the hydrodynamic size. It was shown that both adsorbing multiply charged ions (e.g. pyrophosphate ions) onto the TiO_2 nanoparticle surface and coating quantum dot nanocrystals with polymers (e.g. polyethylene glycol) suppressed agglomeration and stabilized the dispersions. DLVO theory was used to qualitatively understand nanoparticle dispersion stability. A methodology using different ultrasonication techniques (bath and probe) was developed to distinguish agglomerates from aggregates (strong bonds); and to estimate the extent of particle agglomeration. Probe ultrasonication performed better than bath ultrasonication in dispersing TiO_2 agglomerates when sodium pyrophosphate was the stabilizing agent. Commercially available Degussa P25 and in-house synthesized TiO_2 nanoparticles were used to demonstrate identification of aggregated and agglomerated samples.

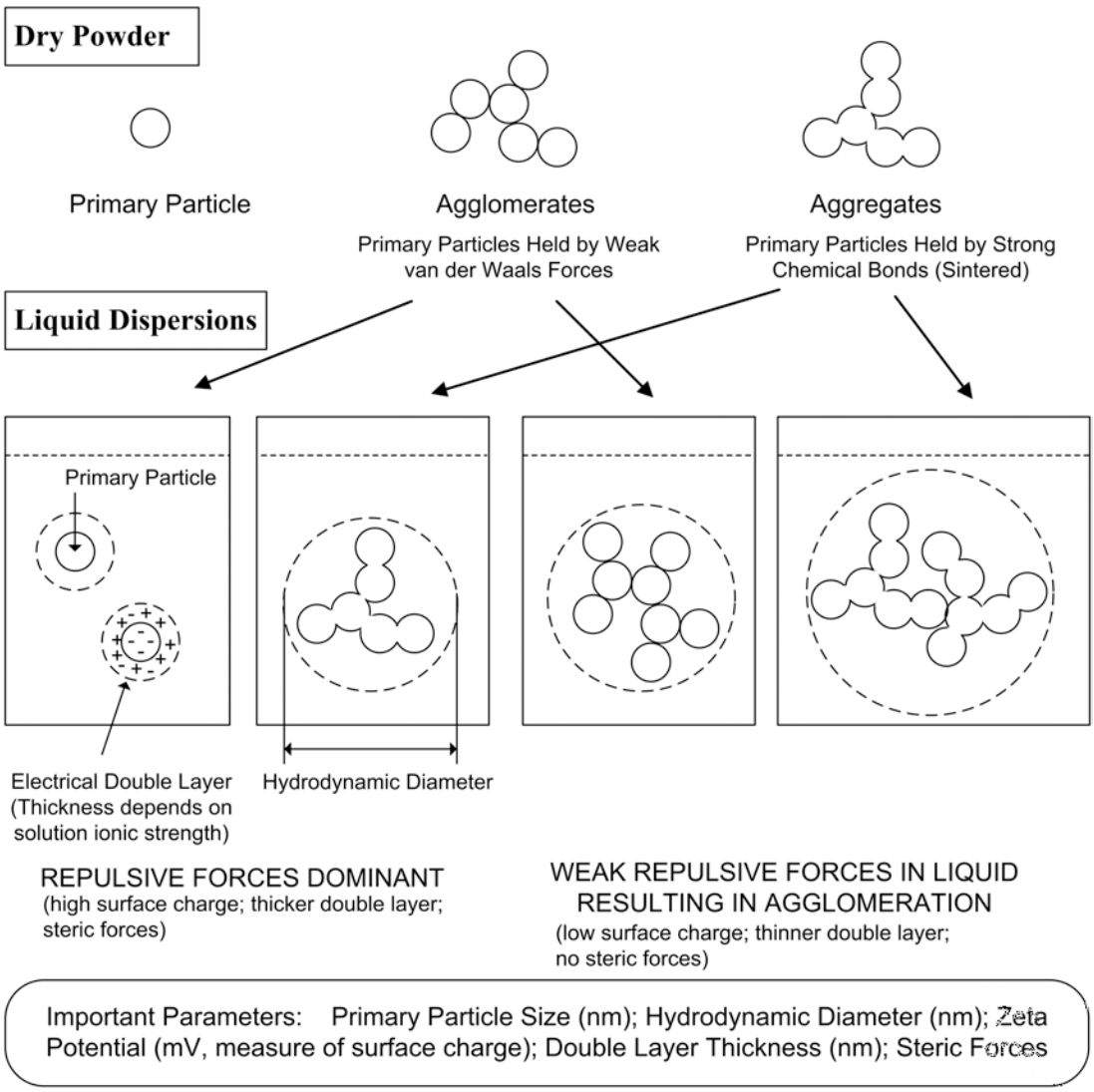

Figure 9 Various states and configurations of particles in dry state and when dispersed in liquids

Nanomaterial suspensions with different dopant types and compositions were also investigated to examine their effects on agglomeration through the measurement of hydrodynamic diameter (HD) and on surface charge and the isoelectric point (IEP) which is important for toxicological investigation as discussed earlier. The nanoparticles all synthesized by flame aerosol reactor considered were pristine TiO_2, Cu-TiO_2, V-TiO_2, and Pt-TiO_2, with dopant concentrations ranging from 1 to 6 wt%. The results indicate that dopant addition can change surface charge and hydrodynamic diameter and also shift the IEP to higher or lower pH than pristine TiO_2, depending on the type of dopant and composition. The effect of pH and copper dopant effect has been shown in the graph which indicates a shift in the iso-electric point (IEP) compared to the pristine TiO_2. Vanadium and platinum doping shifted the IEP to lower pH values, whereas copper doping shifted it to higher pH values. For each of the nanoparticles considered, pH and IS

were found to have significant effects on the surface charge and HD, which were also verified by calculation from DLVO theory. The results suggested that the state of dispersion including physicochemical properties of nanoparticles, pH and ionic strength have to be carefully accounted for.

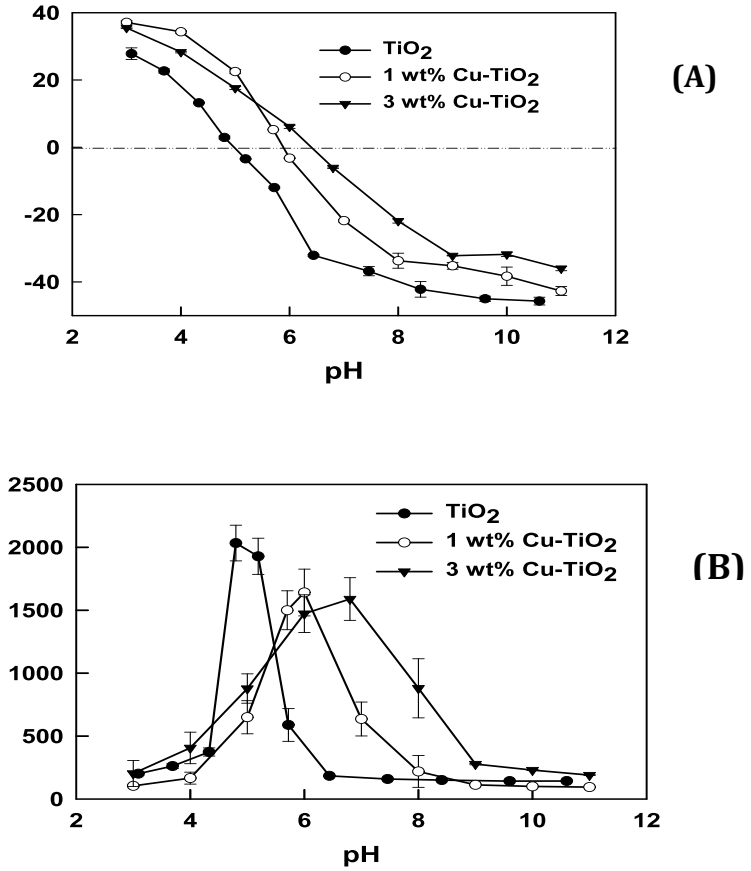

Figure 10. pH and Cu-dopant effects on TiO_2 nanoparticles (A) Zeta potential and (B) Average diameter (Ionic strength=0.001 M NaCl)

Initial ROS studies were done using Cu-doped TiO_2 with different doping concentrations ranging from 0.25–7% and it was found that acellular ROS generation in general is low and does not change with the dopant concentration. The influence of particle size using 3% Cu-doped TiO_2 (such as 10, 35, 50, 100 nm) to find out the size affects oxidative reactivity. The impact of phase ratios (rutile and anatase) on ROS generation will also be evaluated.

(iii) : Electrospray systems for delivery of nanoparticles.

The achievement for the part performed in the Chen's group is primarily focused on the electrospray technique for nanoparticle dispersion. Three types of electrospray systems were developed in full or partial under the financial support of this project. The first one

is the dual-capillary electrospray system. The system allows us to disperse nanoparticle suspension without altering the property of spray liquids. Meanwhile, the system is capable of encapsulating nanoparticles with various coating material. We had also performed the fundamental study on the droplets and spray current produced by the dual-capillary system. The 2nd system is the 10-nozzle electrospray aerosol generator to increase the throughput of a single-capillary electrospray system. With the aerosol generator, we were able to spray nanoparticle suspension with the mass concentration high enough for the nose-only animal exposure study. Along the same line of throughput we (in the collaboration with Pui's group) had further developed a high mass throughput electrospray system capable of dispersing nanoparticles in gas with the mass concentration high enough to perform the whole body animal exposure study. Together with the Pui's group we had also developed the recipe for spraying nanocarbon tubes at the high mass concentration for whole-body animal exposure study. The last system developed for the project is the high transmission single capillary electrospray system. Through the system design change and the optimization process we finally have an electrospray system with the particle transmission efficiency as high as 95% for particles with the size less than 1 micrometer. Note that the 30-40% transmission efficiency is often encountered in existed electrospray systems (including the one commercially available).

Interactions/Transitions

Participation/presentations at meetings, conferences, seminars, etc.

Pratim Biswas, Critical Review Presentation: "Environmental Nanoparticles" Air and Waste Management Association Annual Meeting, June 2005.

Jingkun Jiang and Pratim Biswas, "Theoretical and Experimental Studies of Nanoparticle Charging and Capture", 2005 American Association for Aerosol Research, Austin, Texas, October 2005.

Pratim Biswas, invited talk "Nanoparticle Synthesis for Toxicological Studies", National Institute of Occupational Health and Safety, March 2006.

Jingkun Jiang, Pratim Biswas, Da-Ren Chen, Günter Oberdörster, and Pamela Mercer, "Synthesis of Nanoparticles with Tight Control on Crystallinity, Size and Morphology for Biological Studies", 2006 International Aerosol Conference, September 2006, St. Paul, Minnesota

Christopher J. Hogan Jr., Jingkun Jiang, and Pratim Biswas, "Nanoparticle Charging and Capture in the 6-15nm Size Range with Direct Photoionization and Diffusion Mechanisms: Theory and Experiments", 2006 International Aerosol Conference, September 2006, St. Paul, Minnesota

"Synthesis of Nanoparticles with Tight Control on Size and Other Properties in Flame Aerosol Reactors (FAR) with a Multi-stage DMA System," J. Jiang, D. Chen, P. Biswas, 7th IAC, St. Paul, MN, September 10-15, 2006.

"BSA Coating Gold Nanoparticles in Electrospray Process," F. Mei and D. Chen, 7th IAC, St. Paul, MN, September 10-15, 2006.

Patcharin Worathanakul, Jingkun Jiang, Paisan Kongkachuichay, Pratim Biswas, "Single Step Synthesis of Nanostructured Composite by Flame Aerosol Route", American Chemical Society 233rd National Meeting & Exposition, March 2007, Chicago, Illinois.

"Preparation of Coated Gold Particles by Dual-capillary Electrospraying," F. Mei and D. Chen, AAC, Kaohsiung, Taiwan; August 26-29, 2007

"Dual-capillary Electrospraying for Coated Particle Generation," F. Mei and D. Chen, AAAR 26th Annual Conference, Reno, Nevada, Sept. 24-28, 2007

"Spray Current and Droplet Size in a Dual-capillary Electrospray System," Fan Mei and Da-Ren Chen, AAAR 27th Annual Conference, Rosen Shingle Greek, Orlando, FL, Oct. 20-24, 2008.

Sahu, M., B. Wu, Y.J. Tang, and P. Biswas, Single-step Flame Aerosol Synthesis of Cu-doped TiO2 Nanomaterials and Their Potential Toxicity, AAAR 28th Annual Conference, Minnesota, USA, 2009.

Wu, B., Y. Y., R. Huang, M. Sahu, X. Feng, P. Biswas, and Y.J. Tang, Assessment of Toxicity of Metal Oxide Nanoparticles to Microbial Species, AIChE, USA, 2009.

Huang, R., B. Wu, M. Sahu, X. Feng, P. Wurm, H. Wynder, P. Biswas, and Y.J. Tang, Enhanced Toxicity of Cu-doped TiO2 Nanoparticles to Pathogenic and Environmental Microorganisms, 1st Symposium on Nanotechnology for Public Health, Environment, and Energy. Washington University in St. Louis, 2009.

Sahu, M. and P. Biswas, Single-step processing of Copper-doped Titania Nanomaterials in a Flame Aerosol Reactor, International Aerosol Conference, Finland, 2010.

Sahu, M, B. Wu, L, Zhu, W. N. Wang, Y. J. Tang, and P. Biswas, Role of Nanoparticle Chemical Composition and Particle Size on Toxicity of Cu-doped TiO_2 Nanomaterials in Environmental Microorganism, AAAR 29th Annual Conference, Portland, USA, 2010.

Sahu, M, K. Suttiponparnit, S. Suvachittanont, T. Charinpanitkul, and P. Biswas, Characterization of Doped TiO_2 Nanoparticle Dispersion: The Effect of Dopants, AAAR 29th Annual Conference, Portland,USA, 2010.

Park, J, M. Sahu and P. Biswas, Characterization of In-Situ Charge Distribution of TiO_2 and Cu-Doped-TiO_2 Nanoparticles in a Flame Aerosol Reactor, , AAAR 29th Annual Conference, Portland, USA, 2010.

Wu, B., M. Sahu, C.Jacobson, P. Biswas, and Y.J. Tang, Light-Dependent Antibacterial Properties of Cu-Doped TiO2 Nanoparticles (NPs), AIChE, USA, 2010.

Seders, L. A, M. Sahu, Biswas, P & Fein, J.B, Experimental Study of TiO_2 Nanoparticle Adhesion to Silica and Fe(III) Oxide-coated Silica Surfaces, Goldschmidt Conference, USA, 2010.

Consultative and advisory functions to other laboratories and agencies, especially Air Force and other DoD laboratories:

Prof. Gunter Oberdorster – provides us nanoparticle samples to characterize.
Also, performs biological tests on our synthesized nanoparticles.

Prof. David Pui – electrospraying nanoparticles that are generated.

Prof. Saber Hussain, U.S. Air Force – performs biological tests on our synthesized nanoparticles.

Honors and Awards

Jingkun Jiang (Washington University in St Louis) received a student travel grant to 2006 International Aerosol Conference, awarded by the American Association for Aerosol Research.

Jingkun Jiang (Washington University in St Louis) received a student travel grant to the 3rd International Symposium on Nanotechnology, Occupational and Environmental Health (2007), awarded by the symposium committee

Jingkun Jiang (Washington University in St Louis) received a student travel grant to 2007Aerosol Conference, awarded by the American Association for Aerosol Research.

P. Biswas (Washington University in St Louis) did service on National Academies Panel to Evaluate Roadmap for Nanotoxicology, 2008.

Manoranjan Sahu (Washington University in St Louis) received NSF student travel grant to attend 29th American Association for Aerosol Research (AAAR) conference, 2009.